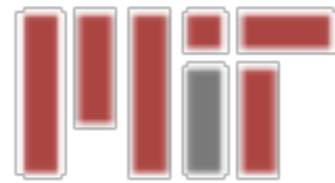




Improving Theoretical Predictions for Gamma-Ray Signals from Heavy WIMPs

Tracy Slatyer



The Dark Side of the Universe DSU '22
UNSW Sydney
9 December 2022

JHEP 1901 (2019) 036, PRD98 123014 (2018), and JHEP 1803 (2018) 117,
with M. Baumgart, T. Cohen, E. Moulin, I. Mout, L. Rinchuso, N. Rodd, M.
Solon, I. Stewart and V. Vaidya

Work to appear with M. Baumgart, N. Rodd, & V. Vaidya

Outline

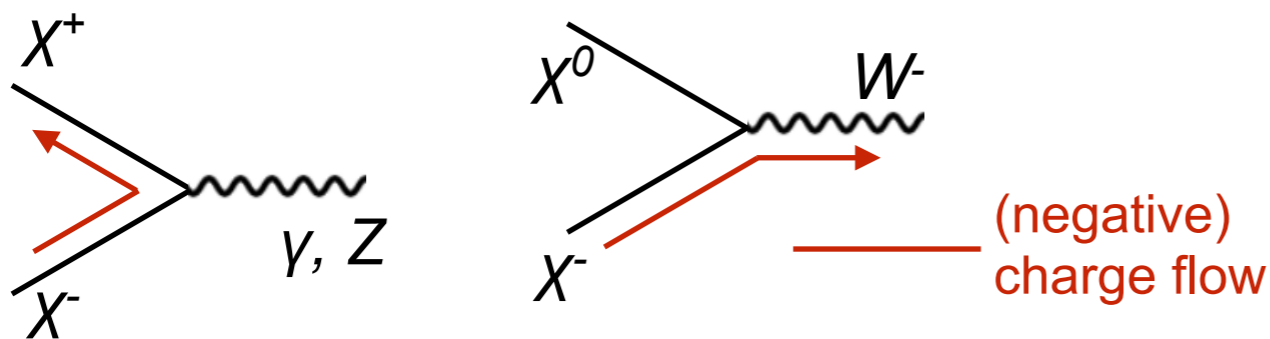
- Minimal heavy WIMPs as a dark matter candidate and testbed for dark sector physics
- Collider/direct constraints (and lack thereof) + the need for indirect detection
- Implications of a large mass hierarchy
 - Nonrelativistic potential effects (Sommerfeld enhancement, bound states)
 - Importance of infrared resummation with effective field theory for annihilation signals
- New (preliminary) results on generalizing the resummation to arbitrary $SU(2)$ representations
- New (preliminary) forecasts and constraint estimates for annihilation of $SU(2)$ quintuplet DM

Dark sectors vs classic WIMPs

- Past decade has seen an enormous flourishing of new ideas for DM, much of it focused on the idea of dark sectors in some form
- In this picture, DM inhabits a new sector that may (or may not) interact with the SM via a mediator particle
- Contrasts with older “classic WIMP” scenario where DM interacts directly with SM weak gauge bosons
- Rich phenomenology - can include DM self-interactions, enhanced scattering/annihilation at low velocities, nearly-degenerate partner particles (e.g. pseudo-Dirac DM), bound states, etc...
- However, classic WIMPs can still be viable - and can actually have similar features to this list, especially if they are heavy

Minimal dark matter (MDM)

- One highly predictive class of scenarios is where DM is charged under the Standard Model weak interactions & transforms as part of a (single) new $SU(2)_L$ multiplet [Cirelli et al '05]
- Neutral component(s) of multiplet are generically lightest; radiative corrections lift the mass of charged partners
- DM interactions with W and Z bosons + number of partner particles are completely fixed by representation of $SU(2)_L$

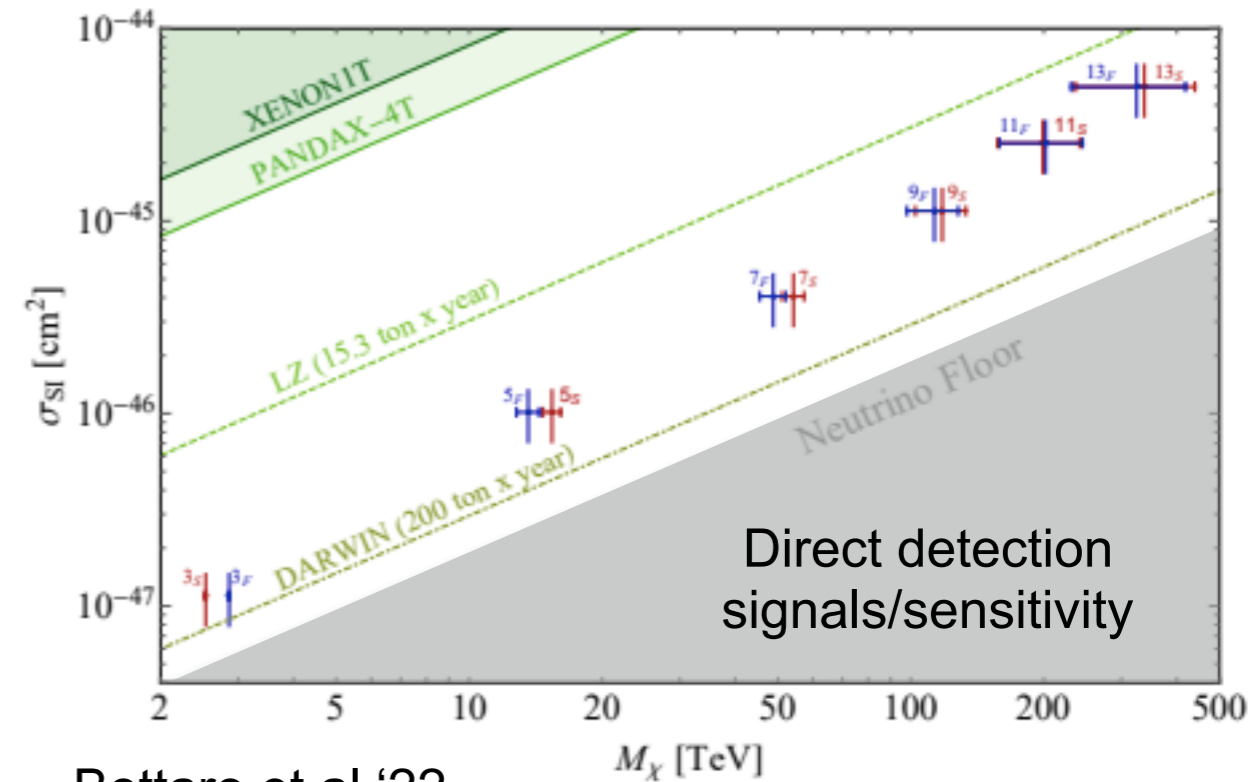


Example in “triplet”
case - DM + two
partners

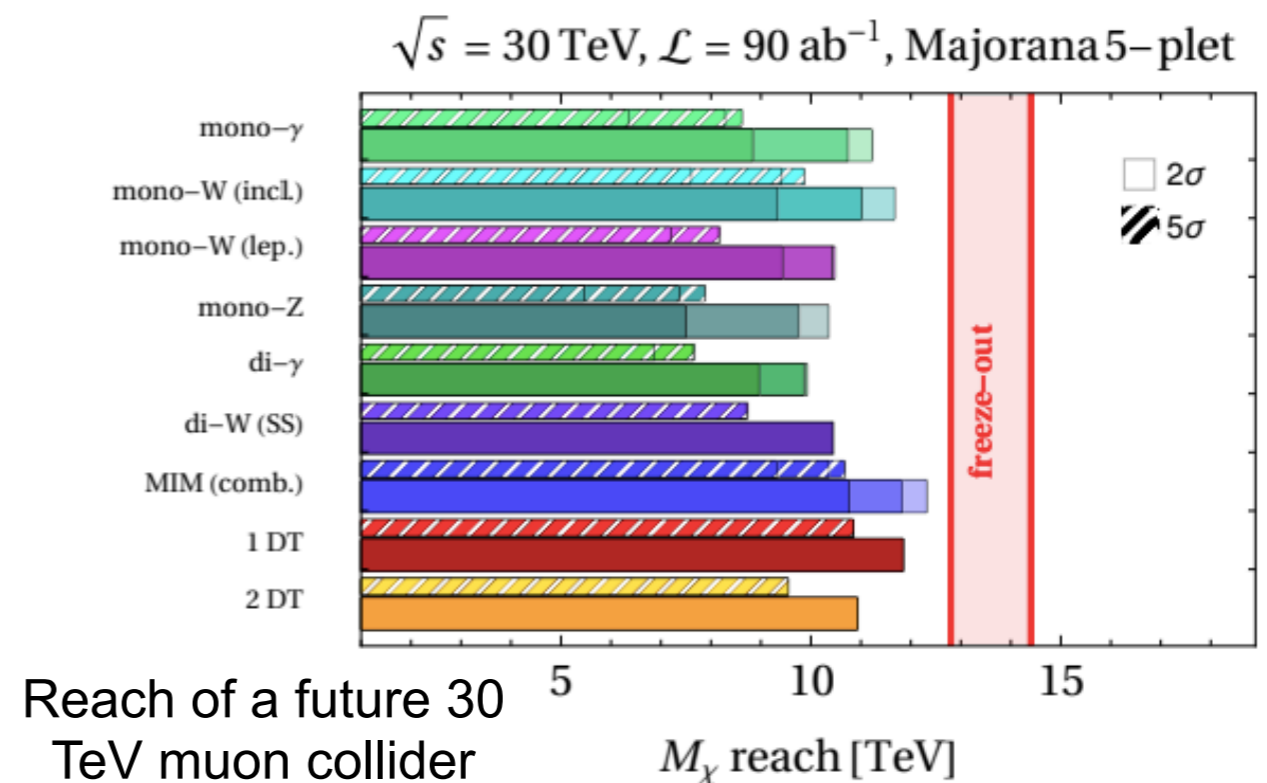
- DM obtains abundance via thermal freezeout - late-time relic density fixed by DM mass once representation + cosmological history are known
- Most-studied examples are doublet & triplet fermions: “pure higgsino” & “pure wino” in SUSY models

Testing minimal dark matter

- Despite being predictive and simple, these models are very hard to exclude!
- Direct detection cross sections are below the reach of LZ/XENONnT (albeit above the neutrino fog - in reach of next-gen experiments)
- High masses needed to explain full DM relic density make collider detection very challenging, although possible for smaller representations or subdominant DM components
- What about indirect detection?

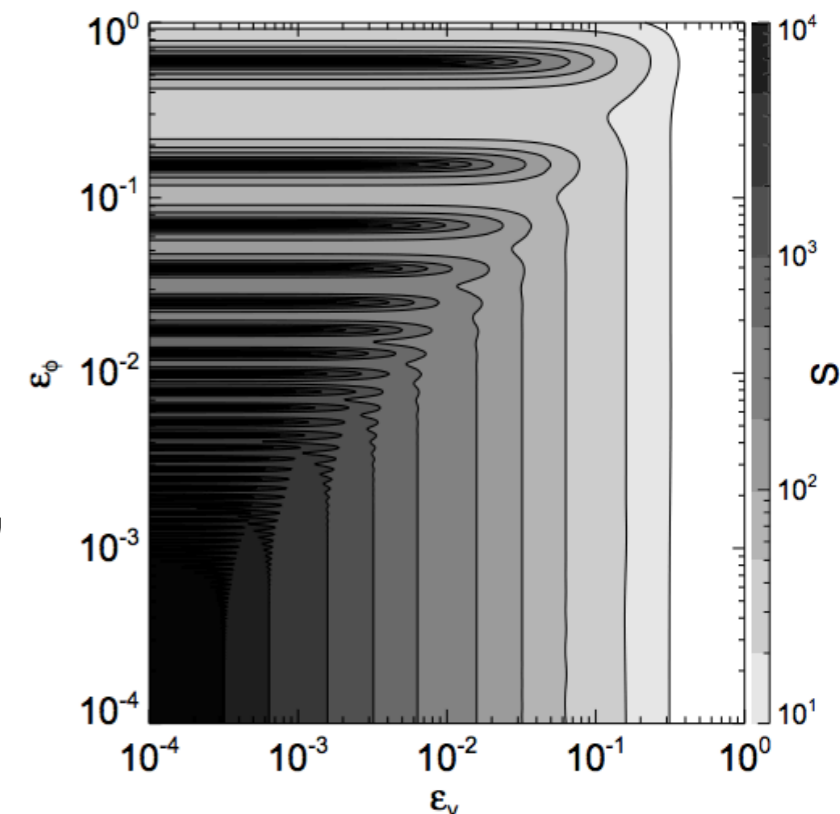
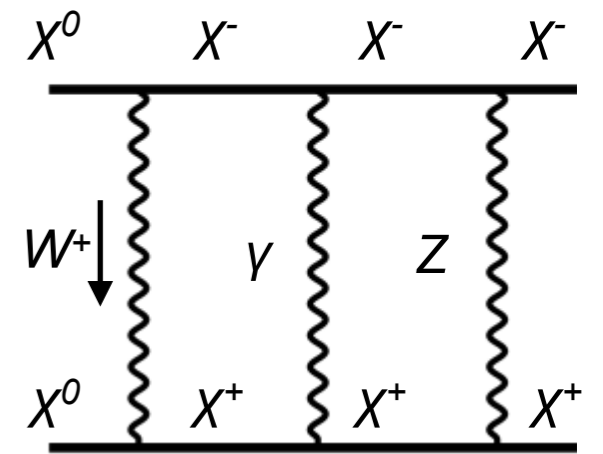


Bottaro et al '22



Long-range potential effects from weak interactions

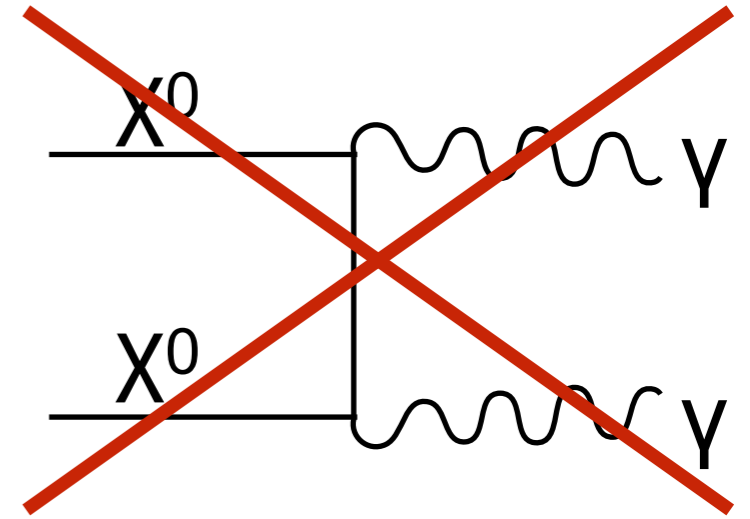
- Exchange of $W/Z/\gamma$'s between particles in multiplet induces potential
- Scale associated with this potential is roughly m_W or inverse Bohr radius $\alpha_W m_{\text{DM}}$, whichever is larger
- Behavior similar to E&M (bound states, large distortions of the 2-body wavefunction) occur for $m_W \lesssim \alpha_W m_{\text{DM}} \Rightarrow m_{\text{DM}} \gtrsim m_W / \alpha_W \sim 3 \text{ TeV}$
- Noted in the form of "Sommerfeld enhancement" annihilation at low velocities (potential energy $>$ kinetic energy, $v \lesssim \alpha_W$) by [Hisano et al '03, '04](#)



Boosting gamma-ray lines with Sommerfeld enhancement

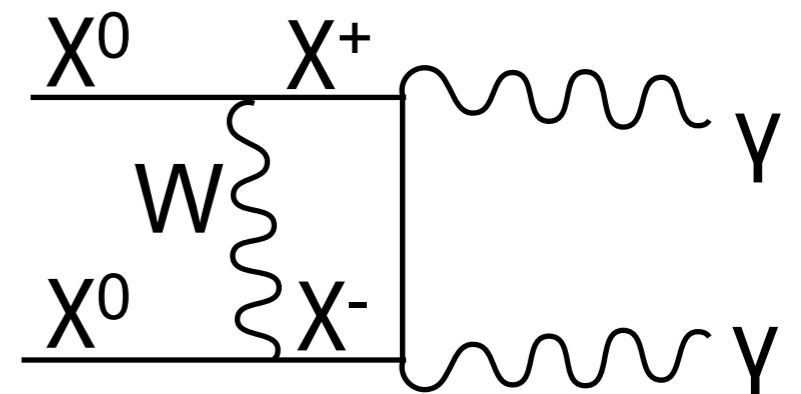
- Sommerfeld enhancement is good for indirect detection in general, but especially for MDM line signals
- Naive expectation: DM doesn't couple directly to photons, so line signal will be loop suppressed and small.
- But Sommerfeld enhancement allows virtual excitation from $\chi_0\chi_0$ to (nearly degenerate) $\chi^+\chi^-$ state. Can annihilate to $\gamma\gamma$, γZ , ZZ with Sommerfeld-enhanced tree-level cross section.
- General lesson: the long-range potential can affect relative detectability of different channels, enhancing line signals if particles in the ladder diagrams are charged.

Forbidden at tree-level

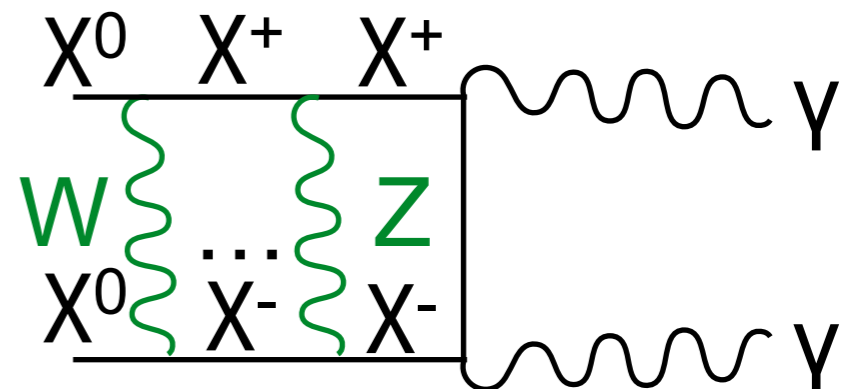


One-loop

$$\sim \sqrt{2} \frac{\alpha_W m_\chi}{m_W}$$

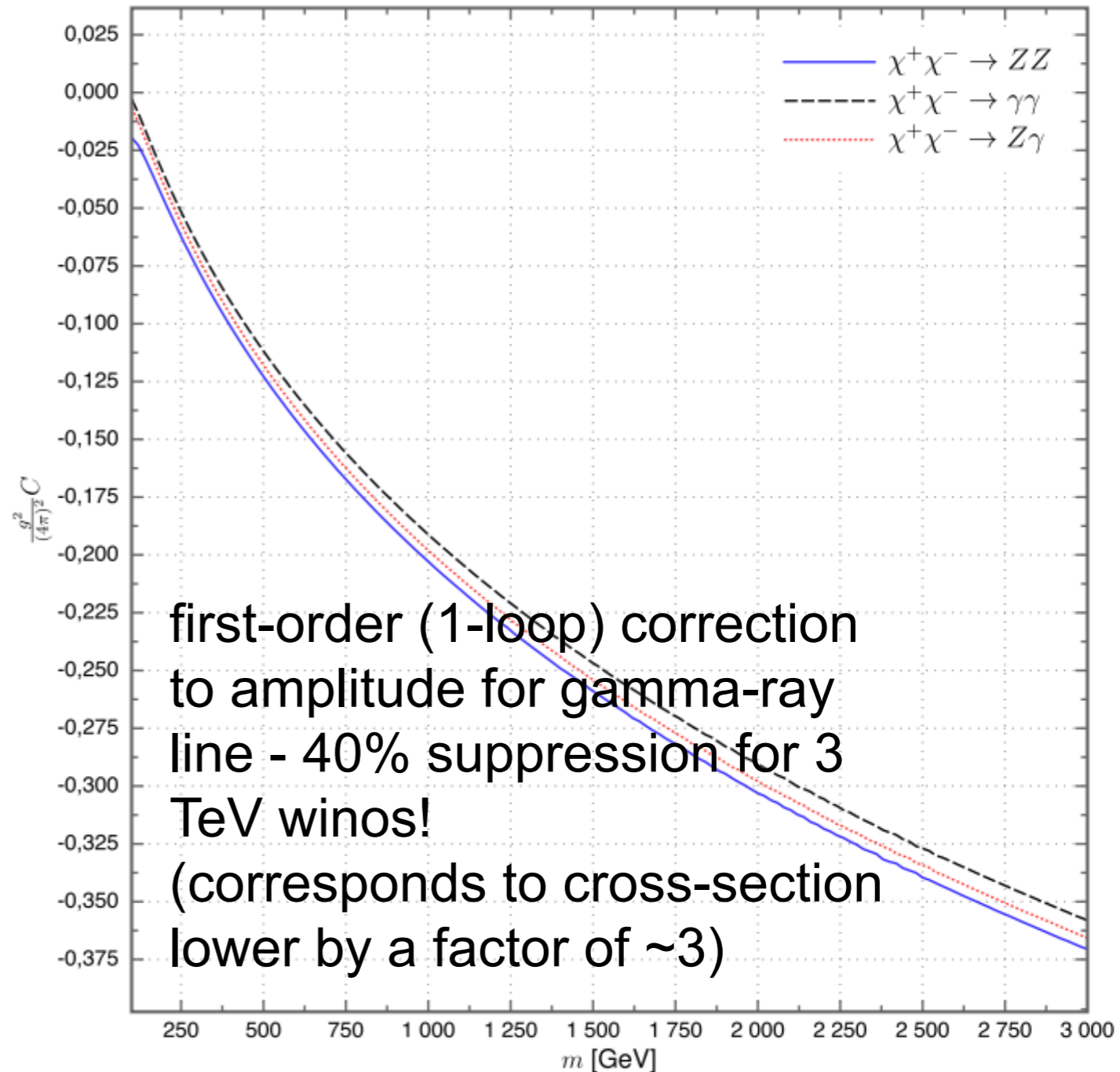


Long-range potential



Large logs from a large mass hierarchy

- Even though coupling is weak, hierarchy of scales in the problem can lead to large effects - theoretically challenging.
- Effects of long-range potential (enhanced annihilation, presence of bound states) can be studied in non-relativistic effective field theory, using Schrodinger equation.
- There are also large corrections arising from infrared behavior.
- Originates from large $\log^2(m_{\text{DM}}/m_W)$ terms that need to be resummed.



Recipe for MDM indirect signals

- Solve the Schrodinger equation to determine:
 - the distortion of the wavefunction of the colliding particles (Sommerfeld enhancement)
 - the spectrum of bound states in the theory

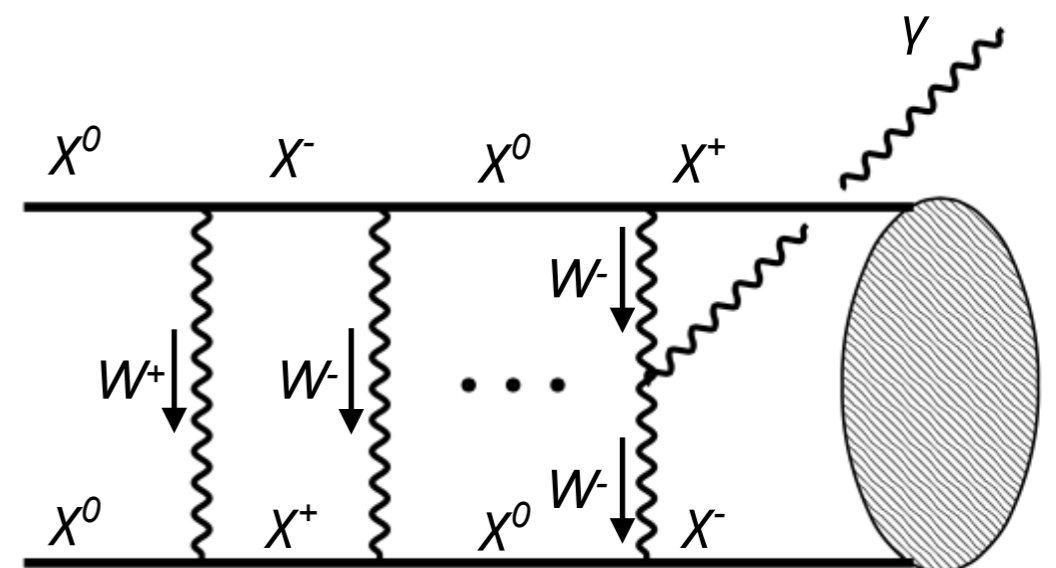
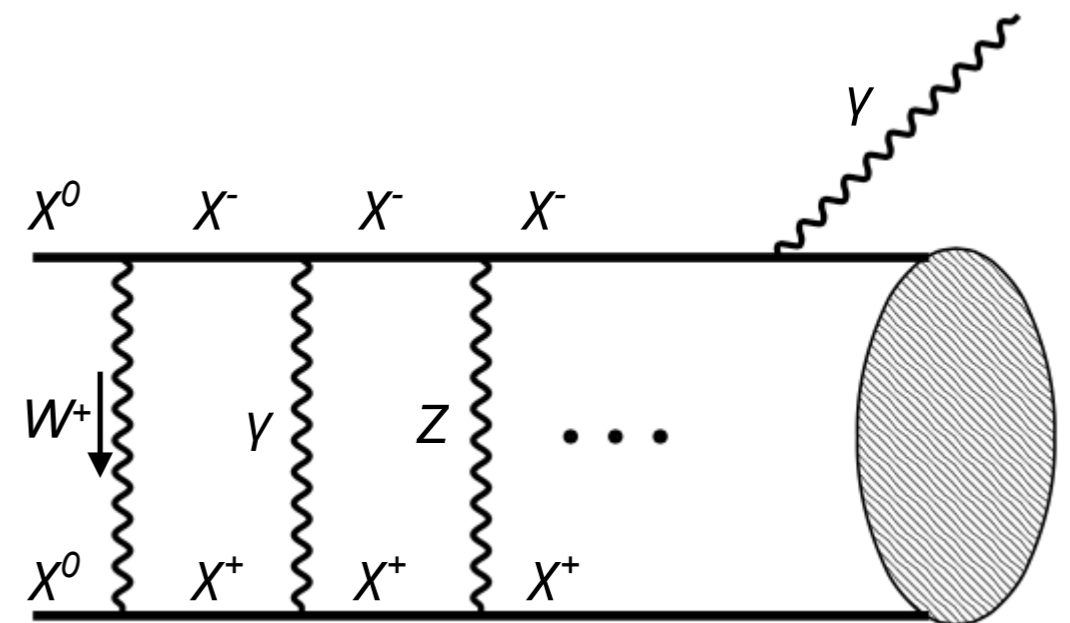
Note: may also need to account for higher-order corrections to the potential, e.g. [Beneke, Szafron & Urban '19](#)
- Use perturbation theory in non-relativistic quantum mechanics to compute the capture rate into bound states and transition rate between bound states, and the resulting spectral lines from these transitions
- Use Soft Collinear Effective Theory (SCET) techniques to compute the annihilation rate of both unbound DM and all the (meta)stable bound states, and the spectrum of gamma rays produced
- The techniques developed here should also be applicable to more general DM scenarios, whenever there is a large mass hierarchy between the DM and particles it interacts with

MDM bound states

Asadi, Baumgart, Fitzpatrick, Krupczak & TRS '16 (erratum '22)

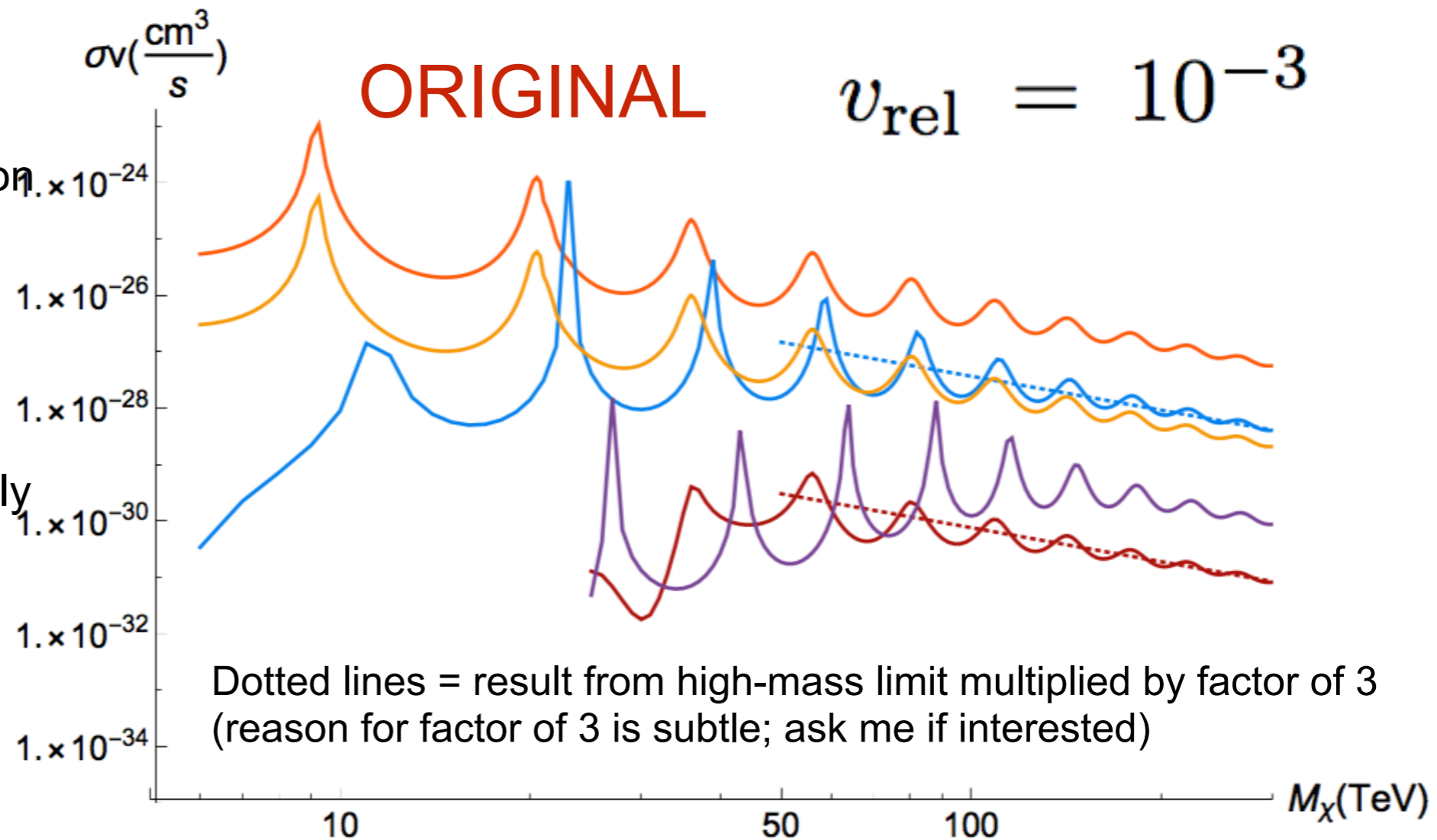
- Bound states are formed radiatively by emission of sufficiently light states (in this case, the photon, + possibly W/Z bosons).
- Selection rules ensure different states have different particle content and potentials - e.g. $L+S$ odd states have symmetric wavefunctions and no $\chi^0\chi^0$ component.
- Because the W boson is itself charged, the bound state can also form by radiating a photon from the potential.
- For heavier DM, formation of charged bound states can dominate, especially for larger representations (higher effective couplings).
- These features - multiple force carriers, bound states mixing different DM-like particles, multiple towers of bound states - are generic for non-Abelian dark sectors.

Formation of “wino-onium”



Example: wino capture rates

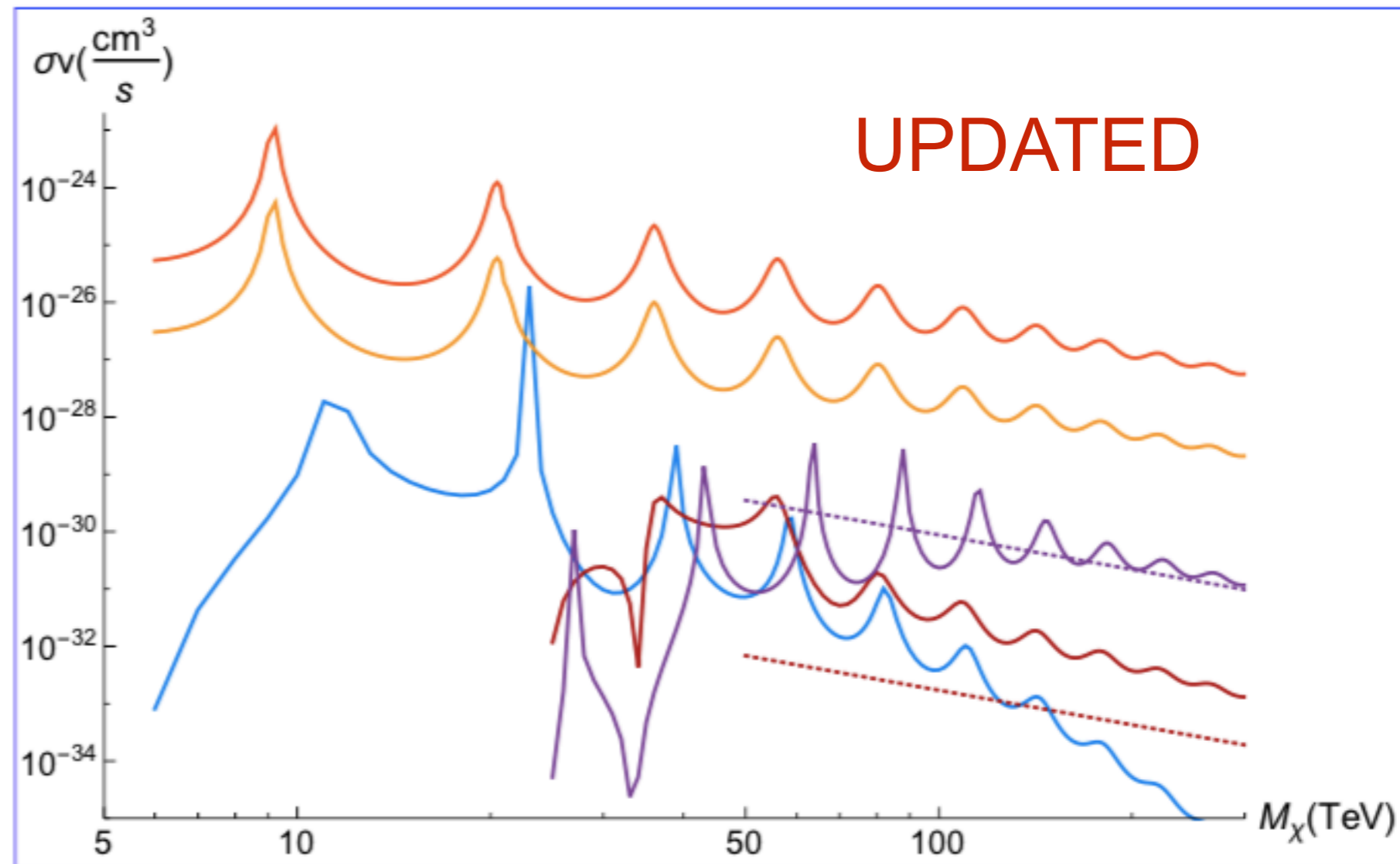
- At the thermal mass, there are no bound states accessible by single-photon capture.
- Even considering higher masses, bound state formation is almost always highly subdominant to annihilation.
- We can understand this analytically in the unbroken-SU(2) limit - differs non-trivially between representations.
- Resonances reflect onset of zero-energy bound states.
- Original paper had a minus sign error - erratum published 2022 (thanks to Julia Harz & Kalliopi Petraki for catching the error!)



Sommerfeld-enhanced inclusive annihilation rate
Sommerfeld-enhanced rate for line photon production
Formation rate of 1S spin-triplet state
s-wave and d-wave contributions to formation of 2P spin-singlet bound states

Example: wino capture rates

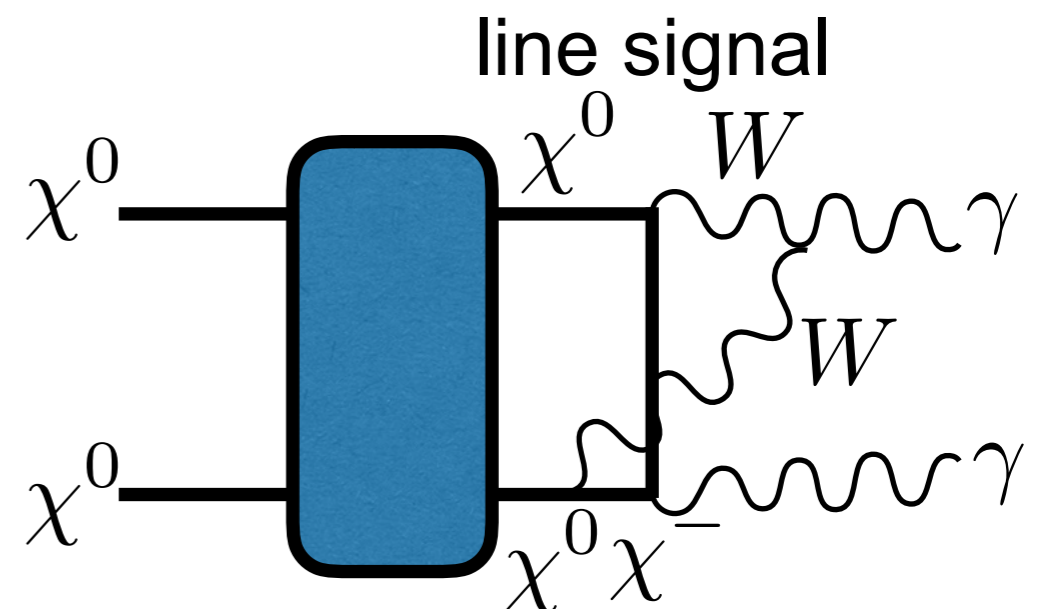
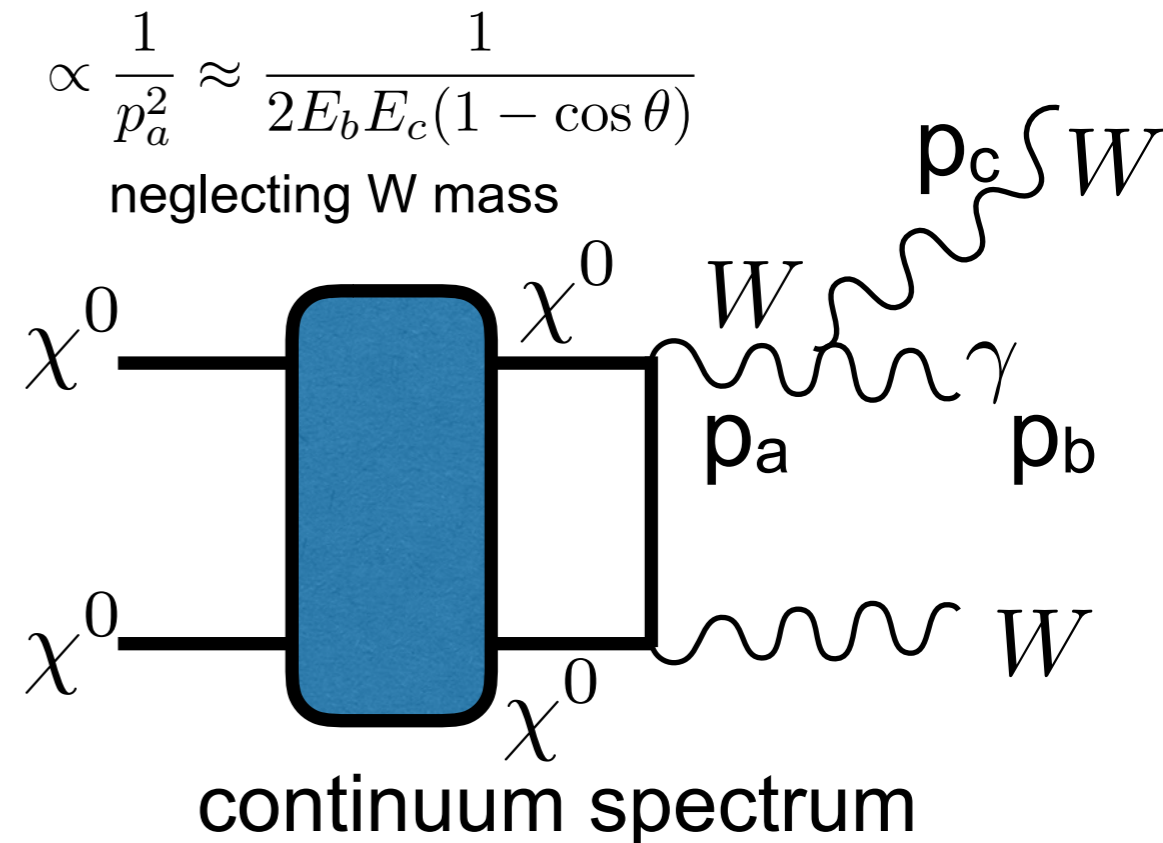
- At the thermal mass, there are no bound states accessible by single-photon capture.
- Even considering higher masses, bound state formation is almost always highly subdominant to annihilation.
- We can understand this analytically in the unbroken-SU(2) limit - differs non-trivially between representations.
- Resonances reflect onset of zero-energy bound states.
- Original paper had a minus sign error - erratum published 2022 (thanks to Julia Harz & Kalliopi Petraki for catching the error!)



Sommerfeld-enhanced inclusive annihilation rate
Sommerfeld-enhanced rate for line photon production
Formation rate of 1S spin-triplet state
s-wave and d-wave contributions to formation of 2P spin-singlet bound states

Resummation with SCET

- Large logs are associated with soft and collinear infrared degrees of freedom
- The same large logs enhance 3-body final states with soft/collinear photons - also needs to be resummed for full photon spectrum
- SCET allows for a convergent perturbative expansion when the coupling is small but $\alpha_W \ln(m_{DM}/m_W)$ becomes $O(1)$



General strategy of SCET

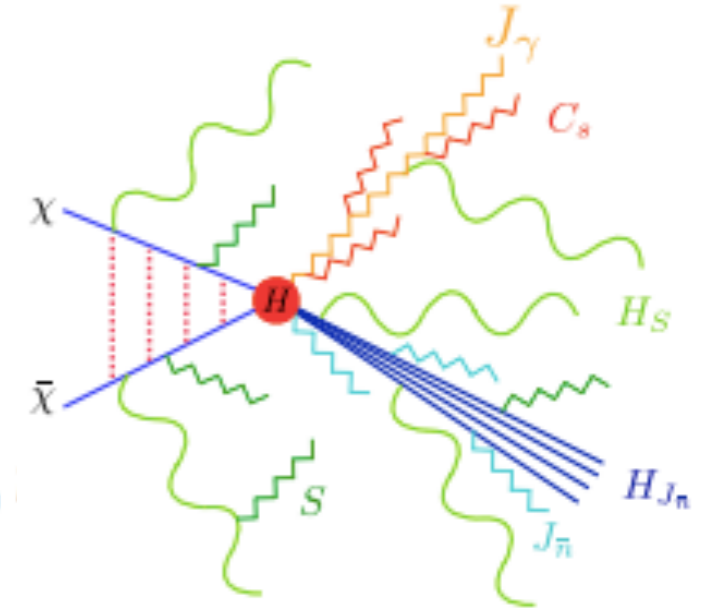
- Match onto full theory (or EFT valid to higher energies) at **high scale**.
- Run operators/fields of interest down to low scale using **renormalization group of EFT** (this captures large logs).
- Match onto desired observables at **low scale**.
- Subtlety for continuum spectrum near endpoint: there are two low scales (m_W and separation from endpoint) - need to run down to higher of these two scales, then match onto a second EFT to complete the evolution. Need **two separate RG evolution steps** (+ matching at **intermediate scale**).

Structure of the resummed result

zigzag = modes sensitive to electroweak symmetry breaking

Baumgart, Cohen, Moulin, Mout, Rinchiuso, Rodd, Solon, TRS, Stewart & Vaidya '19

$$\left(\frac{d\hat{\sigma}}{dz}\right)^{\text{NLL}} = H(M_\chi, \mu) J_\gamma(m_W, \mu, \nu) J_{\bar{n}}(m_W, \mu, \nu) S(m_W, \mu, \nu) \times H_{J_{\bar{n}}}(M_\chi, 1-z, \mu) \otimes H_S(M_\chi, 1-z, \mu) \otimes C_S(M_\chi, 1-z, m_W, \mu, \nu).$$



this is contracted with Sommerfeld factors to get the final result

- We proved a factorization theorem that is valid to NLL, allowing the cross section to be separated into functions describing physics at different scales.

- $H(M_\chi, \mu)$: this hard function captures virtual corrections for $\chi\chi \rightarrow \gamma\gamma, \gamma Z$. do not depend on EWSB, can be evaluated in unbroken theory
- $H_{J_{\bar{n}}}(M_\chi, 1-z, \mu)$: this jet function captures the collinear radiation at the scale $M_\chi\sqrt{1-z}$.
- $H_S(M_\chi, 1-z, \mu)$: this soft function captures soft radiation at the scale $M_\chi(1-z)$.

- $J_\gamma(m_W, \mu, \nu)$: this photon jet function captures the virtual corrections to the outgoing γ .
- $S(m_W, \mu, \nu)$: this soft function captures wide angle soft radiation at the electroweak scale. sensitive to low scale m_W , must be evaluated in broken theory.
- $J_{\bar{n}}(m_W, \mu, \nu)$: this jet function captures collinear radiation in X at the electroweak scale.
- $C_S(M_\chi, 1-z, m_W, \mu, \nu)$: this collinear-soft function captures radiation along the γ direction.

Example: wino annihilation rate

Baumgart, Cohen, Mault, Rodd, Solon, TRS, Stewart & Vaidya '18

$$\frac{d\sigma^{\text{LL}}}{dz} = 4 |s_{0\pm}|^2 \sigma^{\text{tree}} e^{-2\Gamma_0 \tilde{\alpha}_W L_\chi^2} \delta(1-z)$$

$$\sigma = F^{a'b'ab} \hat{\sigma}^{a'b'ab}(z_{\text{cut}})$$

$$+ 4 \sigma^{\text{tree}} e^{-2\Gamma_0 \tilde{\alpha}_W L_\chi^2} \left\{ C_A \tilde{\alpha}_W F_1 \left(3 \mathcal{L}_1^S(z) - 2 \mathcal{L}_1^J(z) \right) e^{2\Gamma_0 \tilde{\alpha}_W \left(\Theta_J L_J^2(z) - \frac{3}{4} \Theta_S L_S^2(z) \right)} \right. \\ \left. - 2 C_A \tilde{\alpha}_W F_0 \mathcal{L}_1^J(z) e^{2\Gamma_0 \tilde{\alpha}_W L_J^2(z)} \right\}. \quad (5.30)$$

$$\Gamma_0 = 4 C_A \quad \tilde{\alpha}_W = \frac{\alpha_W}{4\pi}$$

$$L_J(z) = \log \left(\frac{m_W}{2 M_\chi \sqrt{1-z}} \right) \quad L_S(z) = \log \left(\frac{m_W}{2 M_\chi (1-z)} \right) \quad L_\chi = \log \left(\frac{m_W}{2 M_\chi} \right)$$

$$\Theta_J = \Theta \left(1 - \frac{m_W^2}{4 M_\chi^2} - z \right)$$

$$\Theta_S = \Theta \left(1 - \frac{m_W}{2 M_\chi} - z \right)$$

$$\sigma^{\text{tree}} = \frac{\pi \alpha_W^2 \sin^2 \theta_W}{2 M_\chi^2 v}$$

large logs

$$\mathcal{L}_1^J(z) = \frac{L_J}{1-z} \Theta_J, \quad \mathcal{L}_1^S(z) = \frac{L_S}{1-z} \Theta_S$$

tree-level cross section

power divergences
in (1-z)

$$F_0 = \frac{4}{3} |s_{00}|^2 + 2 |s_{0\pm}|^2 + \frac{2\sqrt{2}}{3} (s_{00} s_{0\pm}^* + s_{00}^* s_{0\pm}),$$

$$F_1 = -\frac{4}{3} |s_{00}|^2 + 2 |s_{0\pm}|^2 - \frac{2\sqrt{2}}{3} (s_{00} s_{0\pm}^* + s_{00}^* s_{0\pm}),$$

Sommerfeld
factors

At NLL, the
power-law terms
are dressed with
additional logs.

Generalizing to larger representations

Baumgart, Rodd, TRS & Vaidya, in progress

- Bound state capture rates and Sommerfeld enhancement need to be re-computed separately for larger representations (at least in the current analysis)
- However, **(preliminarily)** for the SCET calculation it turns out to be possible to separate out the representation information; most of the calculation is unaffected

$$\mathcal{L}_{\text{hard}}^{(0)} = C \left(\chi_v^T i\sigma_2 \left\{ t_\chi^a, t_\chi^b \right\} \chi_v \right) \left(Y^{abcd} \mathcal{B}_{\perp n}^{ic} \mathcal{B}_{\perp \bar{n}}^{jd} \right) i\epsilon^{ijk} (n - \bar{n})^k ,$$

$$C = -\pi \frac{\alpha_W(\mu)}{2M_\chi} ,$$

$$Y^{abcd} = (Y_v^{ae} Y_n^{ce}) \left(Y_v^{bf} Y_{\bar{n}}^{df} \right) .$$

Generalizing to larger representations

Baumgart, Rodd, TRS & Vaidya, in progress

- Bound state capture rates and Sommerfeld enhancement need to be re-computed separately for larger representations (at least in the current analysis)
- However, (preliminarily) for the SCET calculation it turns out to be possible to separate out the representation information; most of the calculation is unaffected

$$\mathcal{L}_{\text{hard}}^{(0)} = C \left(\chi_v^T i\sigma_2 \left\{ t_\chi^a, t_\chi^b \right\} \chi_v \right) \left(Y^{abcd} \mathcal{B}_{\perp n}^{ic} \mathcal{B}_{\perp \bar{n}}^{jd} \right) i\epsilon^{ijk} (n - \bar{n})^k,$$

Depends explicitly on representation of DM particles via generators, contributes to same terms as Sommerfeld factors

$$C = -\pi \frac{\alpha_W(\mu)}{2M_\chi},$$

$$Y^{abcd} = (Y_v^{ae} Y_n^{ce}) \left(Y_v^{bf} Y_{\bar{n}}^{df} \right).$$

controlled solely by physics of adjoint rep (gauge bosons)

Generalizing to larger representations

Baumgart, Rodd, TRS & Vaidya, in progress

- Bound state capture rates and Sommerfeld enhancement need to be re-computed separately for larger representations (at least in the current analysis)
- However, (preliminarily) for the SCET calculation it turns out to be possible to separate out the representation information; most of the calculation is unaffected

$$\mathcal{L}_{\text{hard}}^{(0)} = C \left(\chi_v^T i\sigma_2 \left\{ t_\chi^a, t_\chi^b \right\} \chi_v \right) \left(Y^{abcd} \mathcal{B}_{\perp n}^{ic} \mathcal{B}_{\perp \bar{n}}^{jd} \right) i\epsilon^{ijk} (n - \bar{n})^k,$$

Depends explicitly on representation of DM particles via generators, contributes to same terms as Sommerfeld factors

$$C = -\pi \frac{\alpha_W(\mu)}{2M_\chi},$$

$$Y^{abcd} = (Y_v^{ae} Y_n^{ce}) \left(Y_v^{bf} Y_{\bar{n}}^{df} \right).$$

$$\sigma = F^{a'b'ab} \hat{\sigma}^{a'b'ab}(z_{\text{cut}})$$

controlled solely by physics of adjoint rep (gauge bosons)

can read this off (or trivially re-compute) from SCET wino calculation

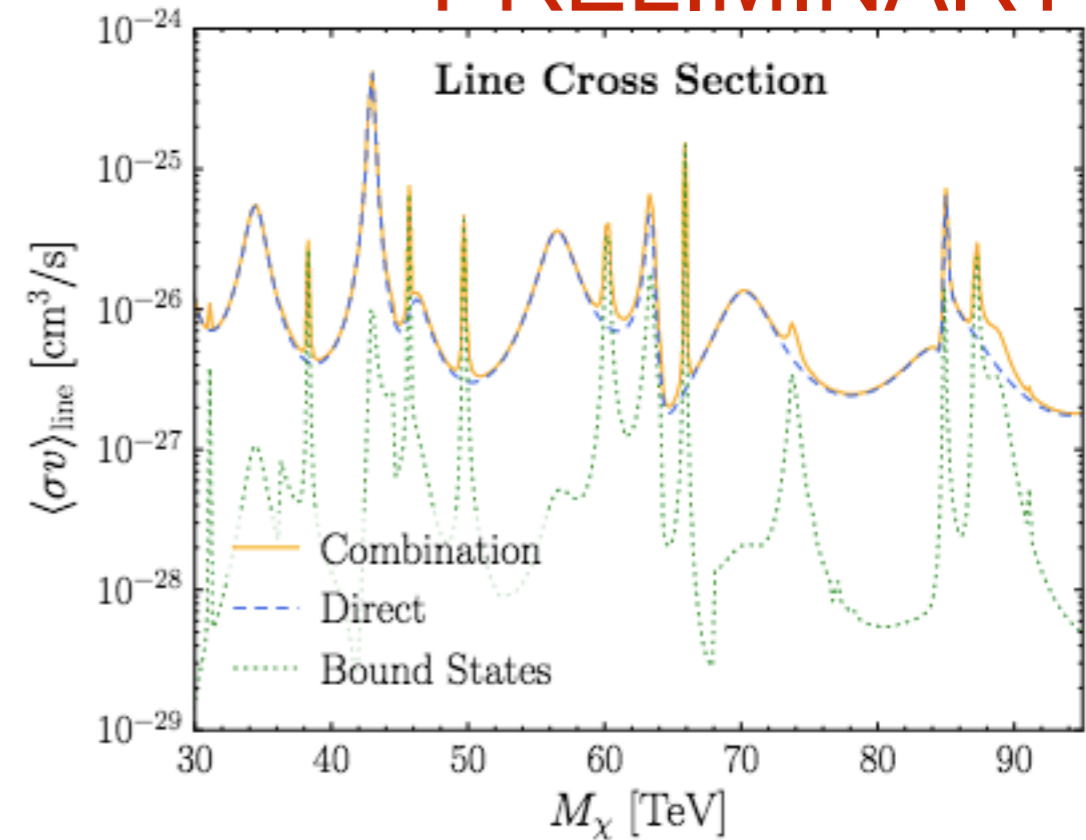
$$F^{a'b'ab} = \langle (\chi^0 \chi^0)_S | \left(\chi_v^T i\sigma_2 \left\{ t_\chi^{a'}, t_\chi^{b'} \right\} \chi_v \right)^\dagger |0\rangle \langle 0| \left(\chi_v^T i\sigma_2 \left\{ t_\chi^a, t_\chi^b \right\} \chi_v \right) |(\chi^0 \chi^0)_S\rangle$$

incorporates Sommerfeld factors & representation dependence from initial state

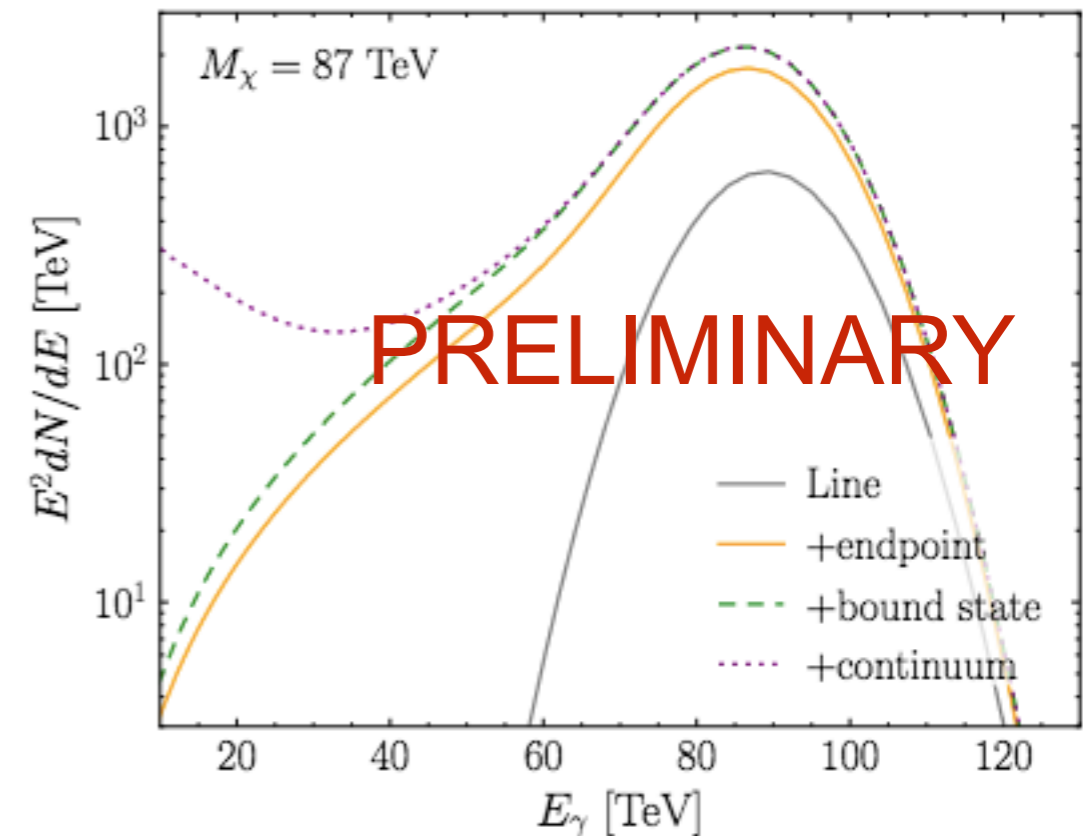
Quintuplet: preliminary results

- In work in progress, we have applied this to the quintuplet representation to determine its gamma-ray spectrum
- Mass to obtain correct relic abundance (with standard cosmology) = 14 TeV
- Bound states turn out to be unimportant for wino DM, but can matter for the quintuplet (although still subdominant at thermal mass)
- We compute formation and decay rates of each of the possible bound states - the resulting signal is substantial at some masses
- Need to account for branching ratio of each bound state to decay to SM vs deeper bound states
- Presence of interfering channels (due to multiple 2-particle states coupled by the potential) can lead to sharp features in the capture rate as a function of mass

PRELIMINARY



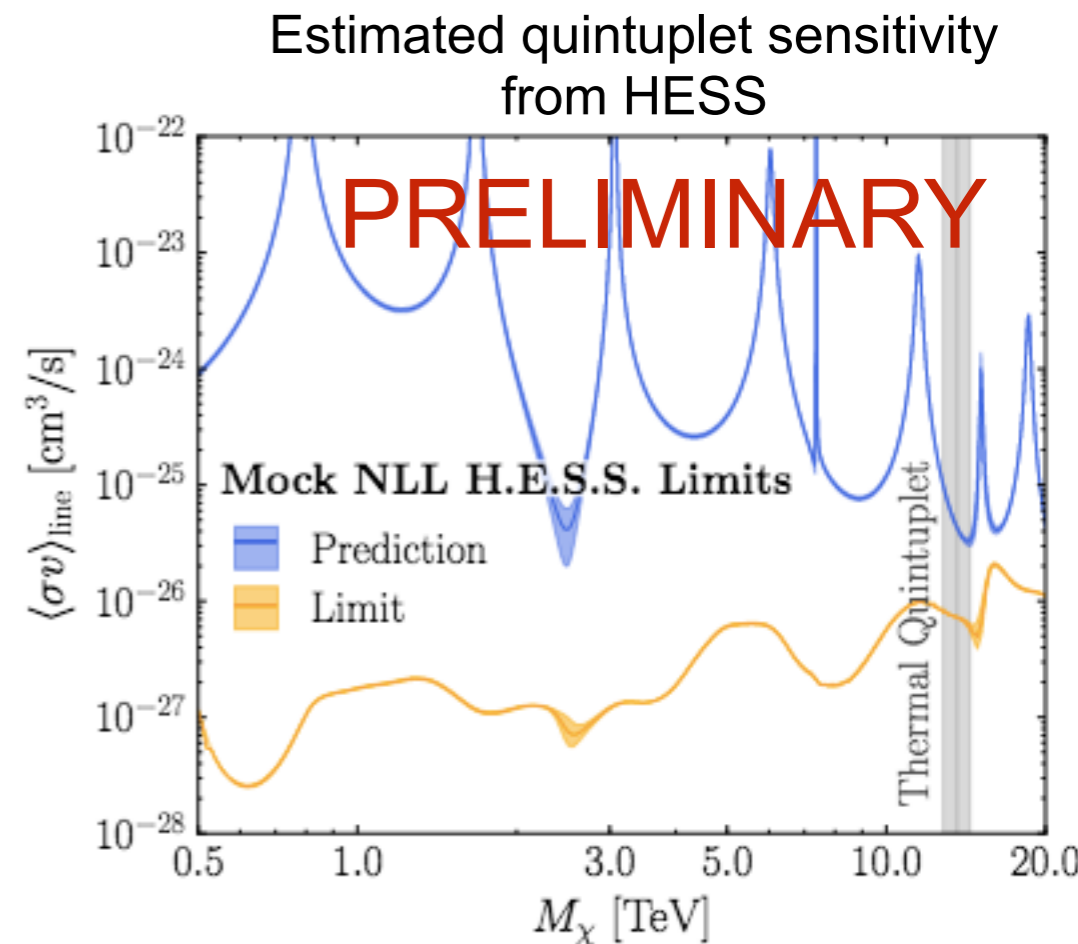
Quintuplet results



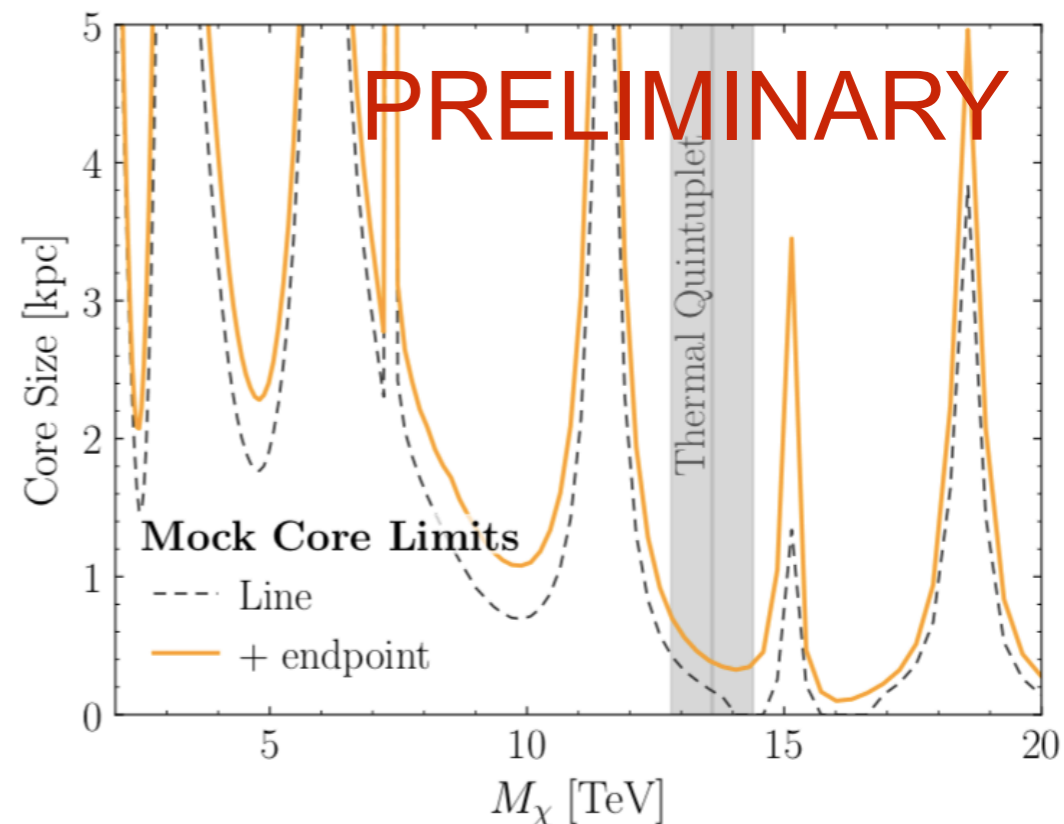
PRELIMINARY

Estimated limits from indirect detection

- We can make a rough estimate of the sensitivity based on older H.E.S.S measurements of the inner Galaxy gamma-ray spectrum
- Consider DM density profiles that are Einasto outside a core radius, with a flat density profile within that radius
- (PRELIMINARY) In this analysis, for the quintuplet, even a small flattened core (<0.5 kpc) would evade detection
- [Montanari et al '22](#) uses our signal prediction with a more sophisticated background model and confirms that in the non-cored case the quintuplet should be detectable by H.E.S.S



Core size needed to evade estimated exclusion



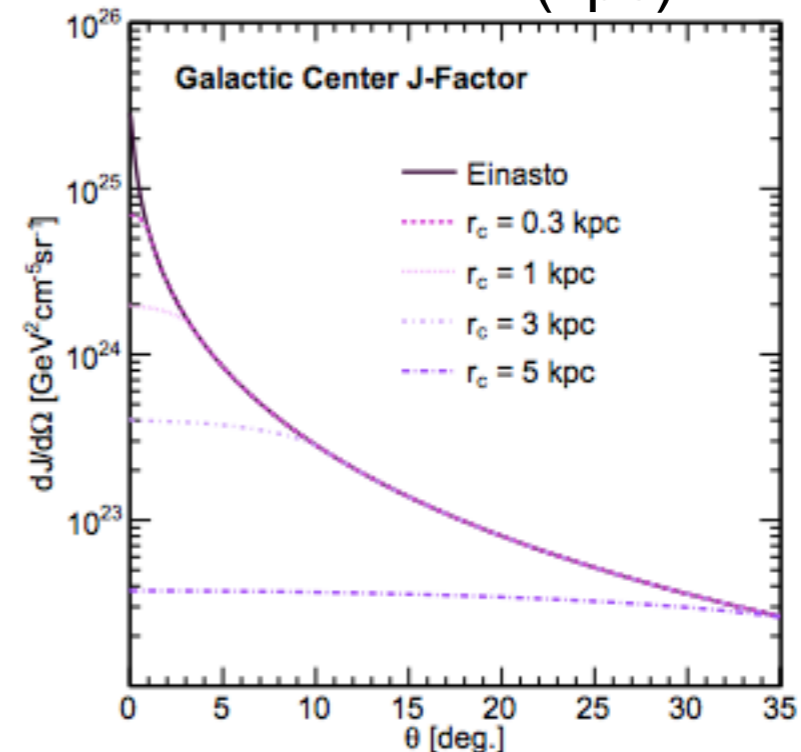
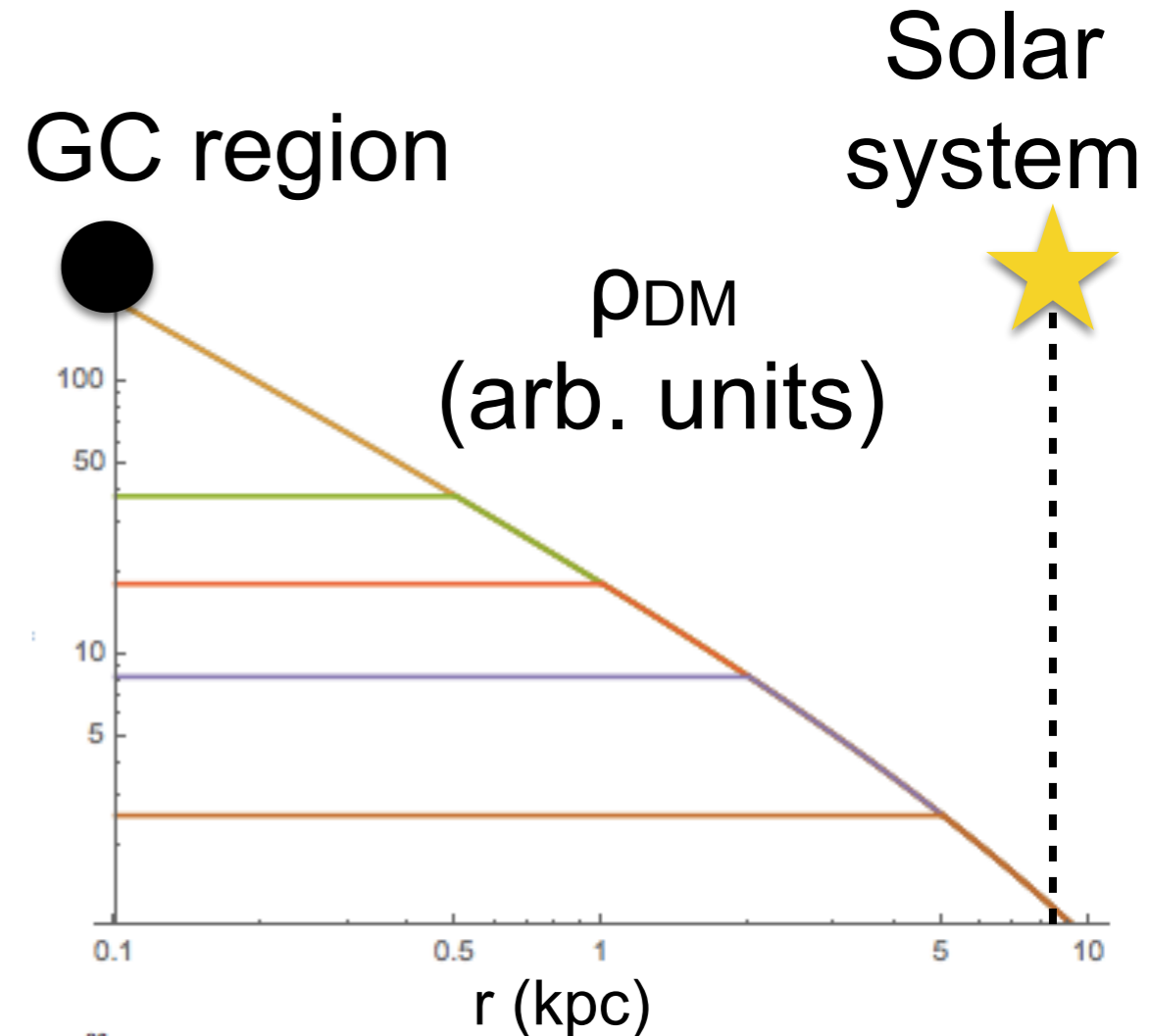
Summary

- Simple, predictive models where DM is in a $SU(2)_L$ multiplet are not yet excluded by colliders or direct detection, and can serve as a testbed for dark sector physics.
- Explaining the full DM relic density with the standard cosmological history requires high ($>TeV$) mass scales in these models.
- At this mass range, weak interactions are effectively long-range: can support bound states and significantly enhance the annihilation cross section.
- Large hierarchy between DM mass and weak scale also leads to large enhancements to loop diagrams from IR effects - need to be resummed.
- We have calculated the hard photon spectrum from heavy $SU(2)_L$ triplet and quintuplet annihilation, including NLL resummation and inclusion of all bound states and their subsequent decays, and worked out a method to generalize this to arbitrary representations.
- Quintuplet appears to be at the edge of detectability with current telescopes - likely ruled out in the case of a NFW/Einasto profile, but tension can be removed by a modestly-sized flat-density core.

BONUS SLIDES

DM density profile

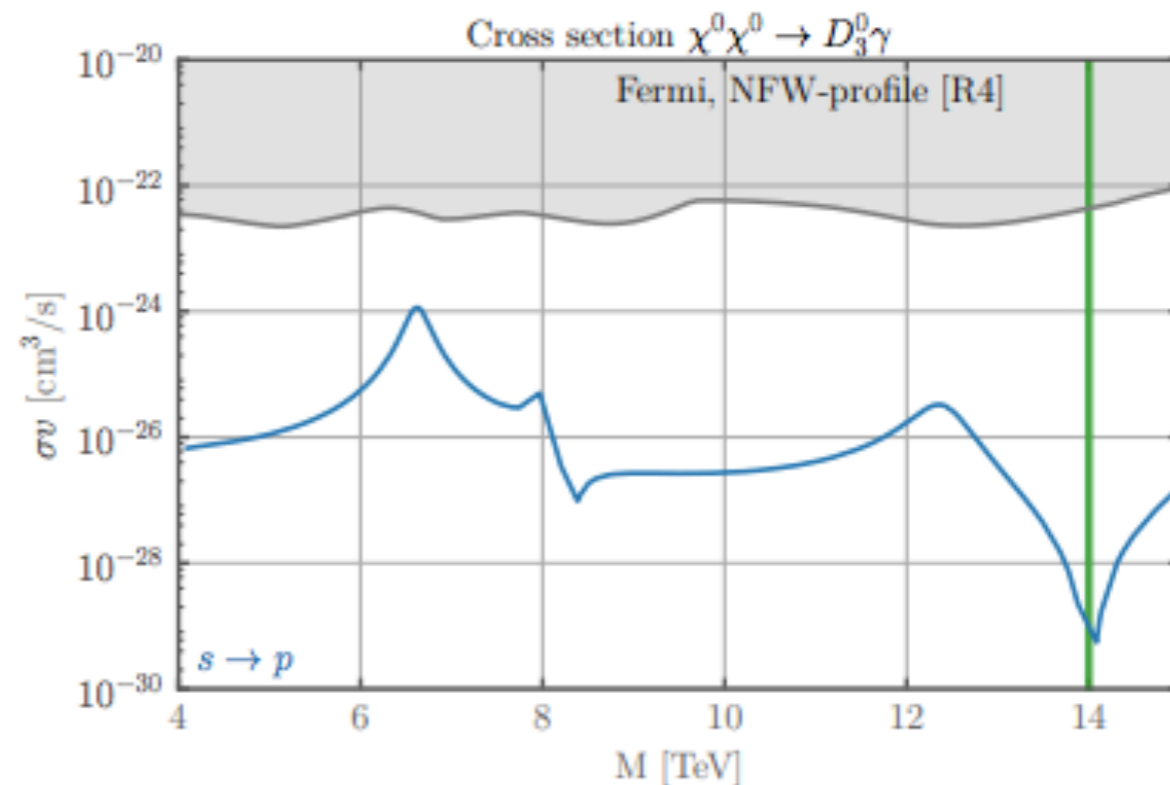
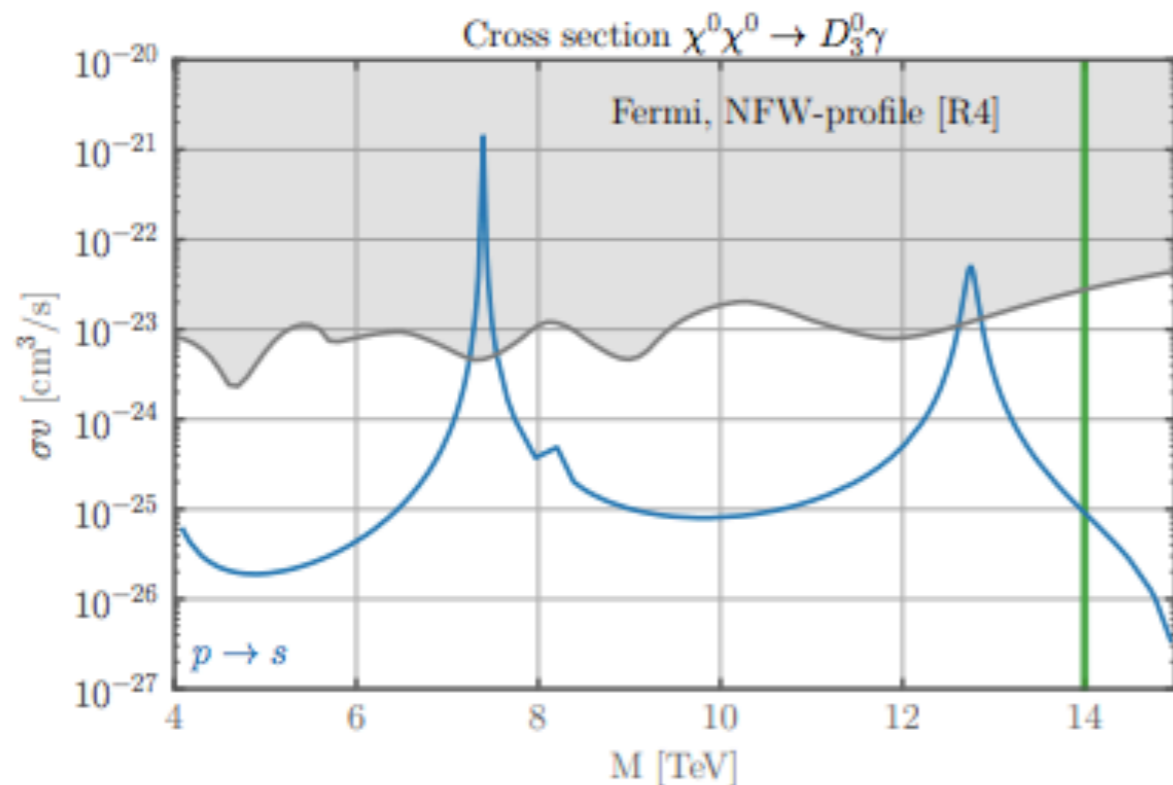
- Limits are really on photon flux - cross section is degenerate with amount of DM near GC, which has large uncertainties
- N-body simulations suggest DM density should rise toward GC (roughly as $1/r$), but flatten out at some “core” radius
- Core size depends on details of baryonic physics - but from current simulations, expected to be ~ 1 -2 kpc or smaller in the Milky Way
- Distance from Earth to GC is ~ 8.5 kpc



can we constrain the “thermal MDM + 1-2 kpc core” scenario?

WIMP spectroscopy?

- Can we see photon emission lines from capture and transitions? Would enable detailed probe of the dark sector
- Such lines would be much lower energy than the DM mass
- Answer based on earlier approximate calculations appears to be “no” for wino/quintuplet with standard thermal mass - 2+ orders of magnitude below current bounds - but potentially more optimistic for modified cosmological histories leading to different thermal masses



Example: the wino bound state spectrum (high-mass)

Spin-Singlet Spectrum

Spin-Triplet Spectrum

$$\left| \frac{E_n}{M_\chi \alpha_W^2} \right| = \frac{1}{144}$$

$$\left| \frac{E_n}{M_\chi \alpha_W^2} \right| = \frac{1}{100}$$

$$\left| \frac{E_n}{M_\chi \alpha_W^2} \right| = \frac{1}{64}$$

$$\left| \frac{E_n}{M_\chi \alpha_W^2} \right| = \frac{1}{36}$$

$$\left| \frac{E_n}{M_\chi \alpha_W^2} \right| = \frac{1}{25}$$

$$\left| \frac{E_n}{M_\chi \alpha_W^2} \right| = \frac{1}{16}$$

$$\left| \frac{E_n}{M_\chi \alpha_W^2} \right| = \frac{1}{9}$$

$$\left| \frac{E_n}{M_\chi \alpha_W^2} \right| = \frac{1}{4}$$

$$\left| \frac{E_n}{M_\chi \alpha_W^2} \right| = 1$$

4S 4P 4D

3S 3P 3D

2S 2P

1S

4S 4P 4D

3S 3P 3D

2S 2P

1S

Example: the wino bound state spectrum (high-mass)

Spin-Singlet Spectrum

Spin-Triplet Spectrum

$$\left| \frac{E_n}{M_\chi \alpha_W^2} \right| = \frac{1}{144}$$

$$\left| \frac{E_n}{M_\chi \alpha_W^2} \right| = \frac{1}{100}$$

$$\left| \frac{E_n}{M_\chi \alpha_W^2} \right| = \frac{1}{64}$$

$$\left| \frac{E_n}{M_\chi \alpha_W^2} \right| = \frac{1}{36}$$

$$\left| \frac{E_n}{M_\chi \alpha_W^2} \right| = \frac{1}{25}$$

$$\left| \frac{E_n}{M_\chi \alpha_W^2} \right| = \frac{1}{16}$$

$$\left| \frac{E_n}{M_\chi \alpha_W^2} \right| = \frac{1}{9}$$

$$\left| \frac{E_n}{M_\chi \alpha_W^2} \right| = \frac{1}{4}$$

$$\left| \frac{E_n}{M_\chi \alpha_W^2} \right| = 1$$

4P

3P

4S 4D 2P

3S 3D

2S

1S

4S 4P 4D

3S 3P 3D

2S 2P

1S

Example: the wino bound state spectrum (high-mass)

Spin-Singlet Spectrum

Spin-Triplet Spectrum

$$\left| \frac{E_n}{M_\chi \alpha_W^2} \right| = \frac{1}{144}$$

$$\left| \frac{E_n}{M_\chi \alpha_W^2} \right| = \frac{1}{100}$$

$$\left| \frac{E_n}{M_\chi \alpha_W^2} \right| = \frac{1}{64}$$

$$\left| \frac{E_n}{M_\chi \alpha_W^2} \right| = \frac{1}{36}$$

$$\left| \frac{E_n}{M_\chi \alpha_W^2} \right| = \frac{1}{25}$$

$$\left| \frac{E_n}{M_\chi \alpha_W^2} \right| = \frac{1}{16}$$

$$\left| \frac{E_n}{M_\chi \alpha_W^2} \right| = \frac{1}{9}$$

$$\left| \frac{E_n}{M_\chi \alpha_W^2} \right| = \frac{1}{4}$$

$$\left| \frac{E_n}{M_\chi \alpha_W^2} \right| = 1$$

4S 4D 2P

3S 3D

2S

1S

4P

3P

4P 2S

3P

2P 1S

4S 4D

3S 3D

Example: the wino bound state spectrum (high-mass)

Spin-Singlet Spectrum

Spin-Triplet Spectrum

$$\left| \frac{E_n}{M_\chi \alpha_W^2} \right| = \frac{1}{144}$$

$$\left| \frac{E_n}{M_\chi \alpha_W^2} \right| = \frac{1}{100}$$

$$\left| \frac{E_n}{M_\chi \alpha_W^2} \right| = \frac{1}{64}$$

$$\left| \frac{E_n}{M_\chi \alpha_W^2} \right| = \frac{1}{36}$$

$$\left| \frac{E_n}{M_\chi \alpha_W^2} \right| = \frac{1}{25}$$

$$\left| \frac{E_n}{M_\chi \alpha_W^2} \right| = \frac{1}{16}$$

$$\left| \frac{E_n}{M_\chi \alpha_W^2} \right| = \frac{1}{9}$$

$$\left| \frac{E_n}{M_\chi \alpha_W^2} \right| = \frac{1}{4}$$

$$\left| \frac{E_n}{M_\chi \alpha_W^2} \right| = 1$$

5P

4P

3P 6D

5D

4S 2P 4D

3S 3D

2S

1S

6D

5D

4S 4D

3S 3D

5P

2S 4P

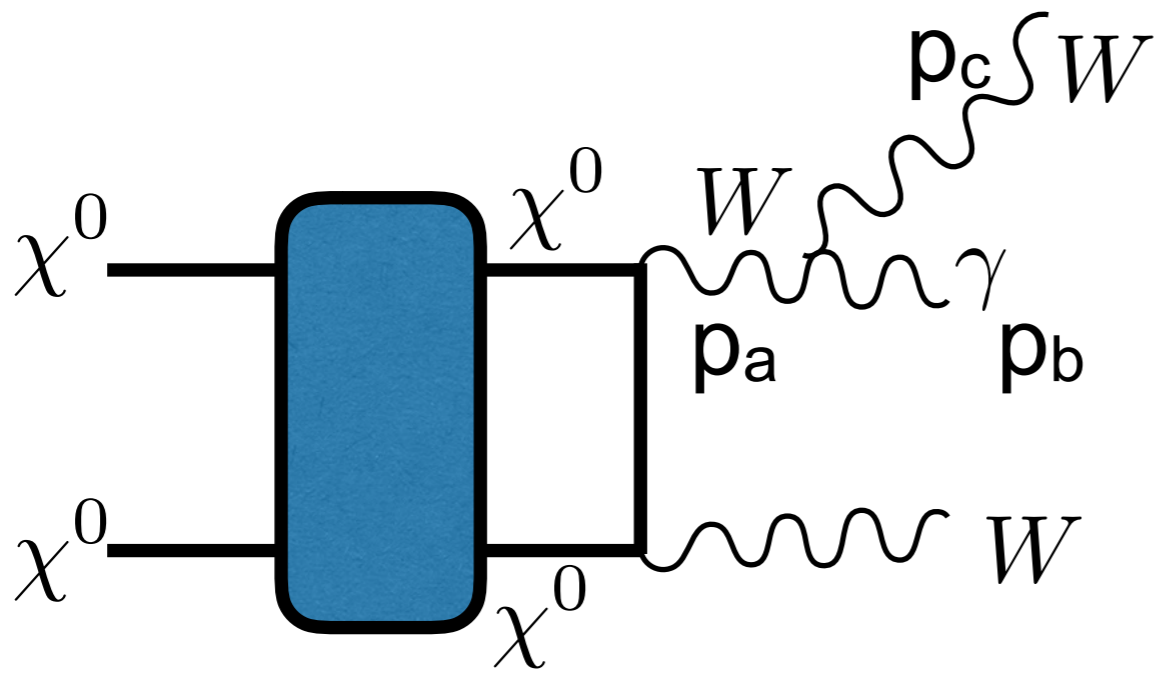
3P

1S 2P

- Spectrum + decays of bound states are quite different to hydrogen/positronium
- Modifies which states are metastable, & energy gaps between states

Infrared divergences

- Consider final states including at least one photon, visible to telescopes. In particular, consider photon- W^+W^- final state, produced at tree level.
- Soft radiation: radiate low-energy particles from final state, $E \ll m_\chi$.
- Collinear radiation: narrow splitting of one particle into two, small angle θ between particles.
- In the limit where W is massless, these parts of phase space produce infrared divergences.
- Canceled by corresponding IR divergence in one-loop diagrams with two-particle final state.

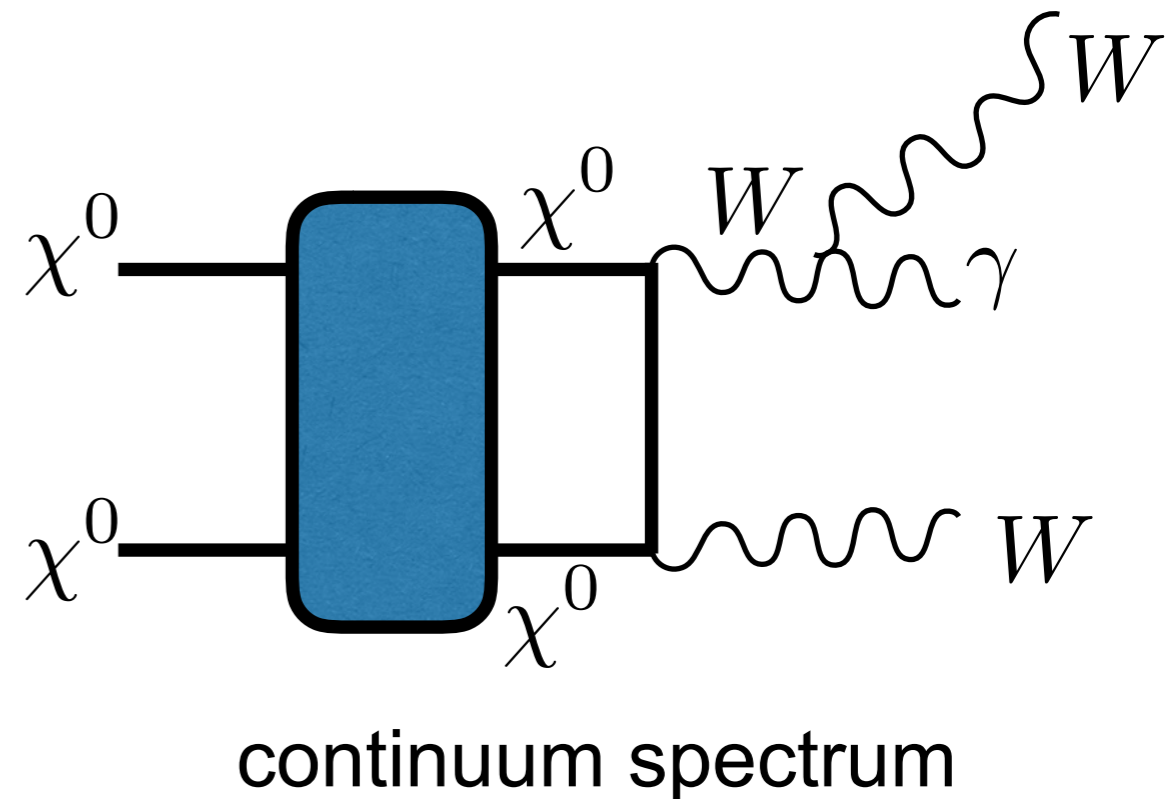
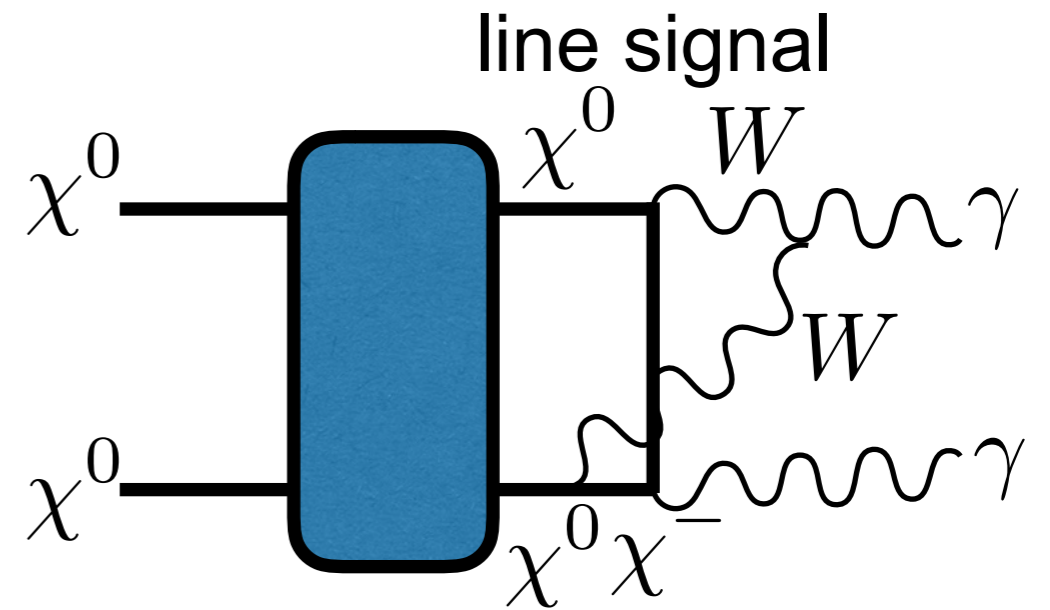


$$\propto \frac{1}{p_a^2} \approx \frac{1}{2E_b E_c (1 - \cos \theta)}$$

neglecting W mass

The origin of large logs

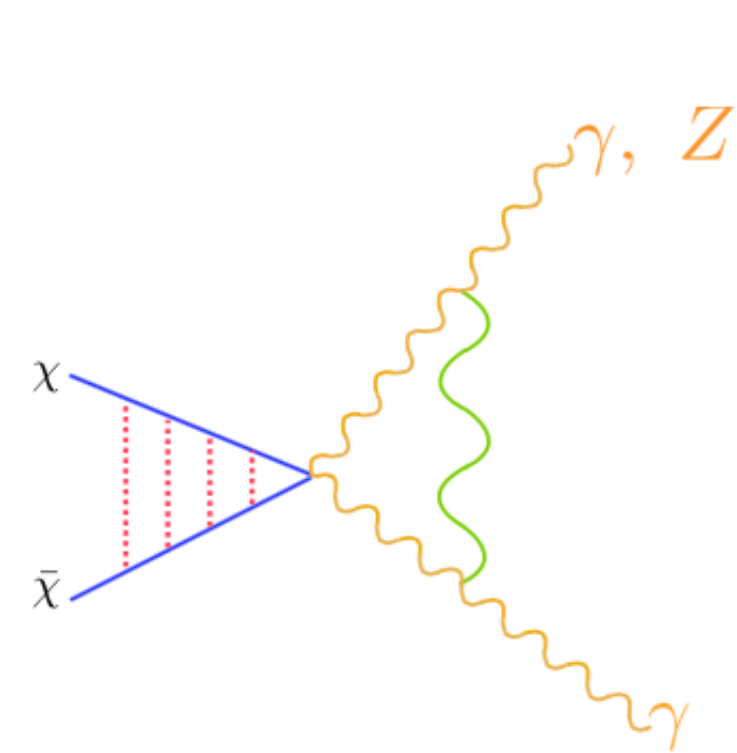
- Once a mass for the W is turned on, it regulates these IR divergences, but both kinds of diagrams (2-body and 3-body final states) still have large log-enhanced contributions, $\alpha_w \ln^2(m_\chi/m_W)$.
- Need to resum logs for reliable results.
- Need to account for enhanced 3-body final state - calculate full photon spectrum, not just line.
- In this case, logs of another small scale appear - the separation between the photon energy and the endpoint of the spectrum at $E_\gamma = m_\chi$.



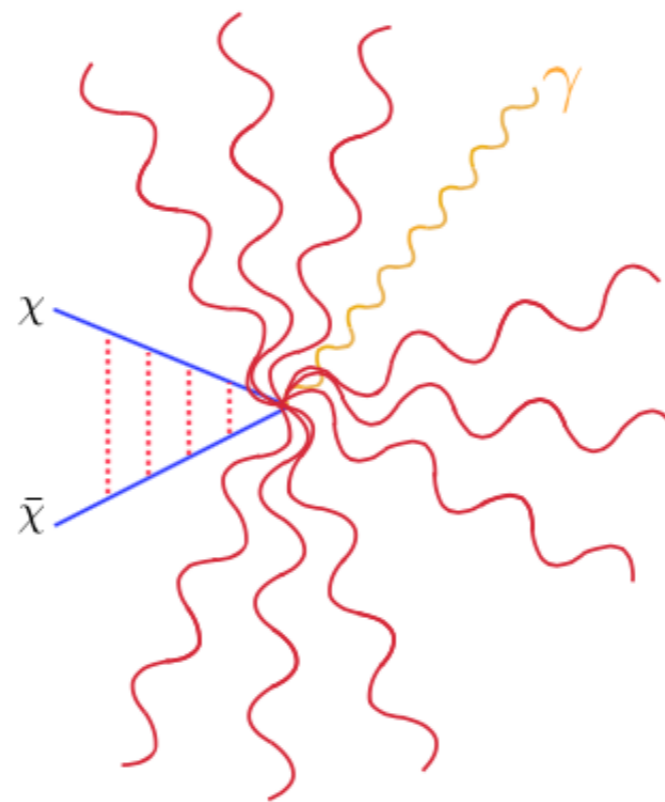
Three regions

$$z \equiv E_\gamma / m_\chi$$

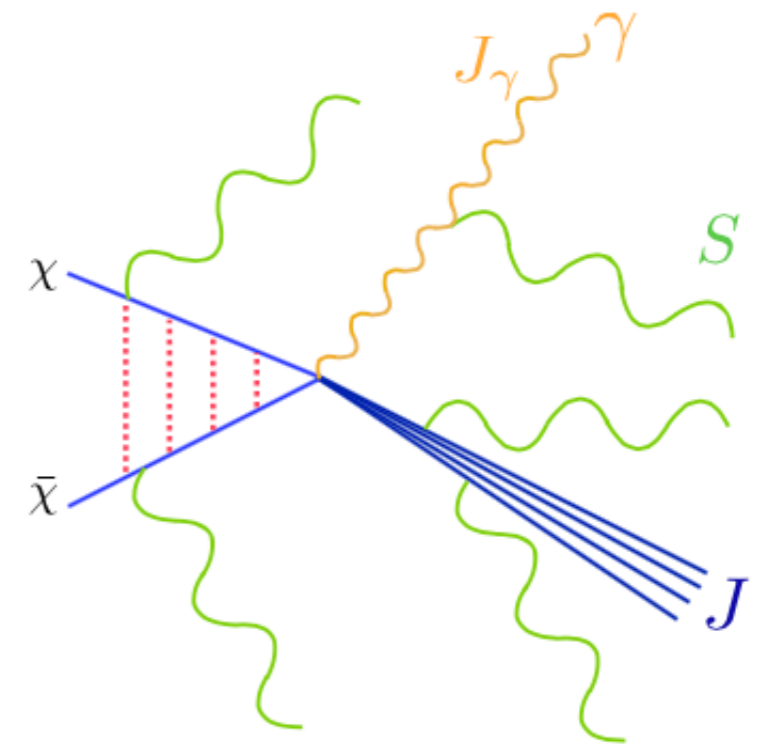
$$m_X^2 = 4m_\chi^2(1 - z)$$



(a)



(b)



(c)

Exclusive

2→2 annihilation

$\gamma\gamma$, γZ final states

Cohen et al '15; Ovanesyan, TRS & Stewart '15; Ovanesyan, Rodd, TRS & Stewart '17

Semi-inclusive

Integrate out recoil state X

$\gamma+X$ final state, X heavy

Baumgart et al '15a,b; Baumgart & Vaidya '16

Endpoint region

Recoil state forced into jet

$\gamma+X$ final state

Baumgart, TRS et al, '18,'19

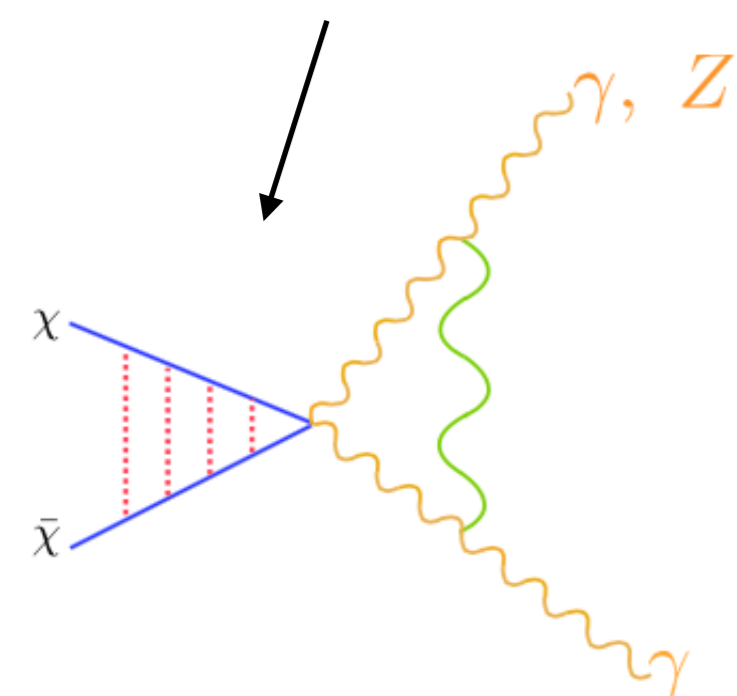
For the regime even closer to the endpoint, see Beneke et al '18,'19

Three regions

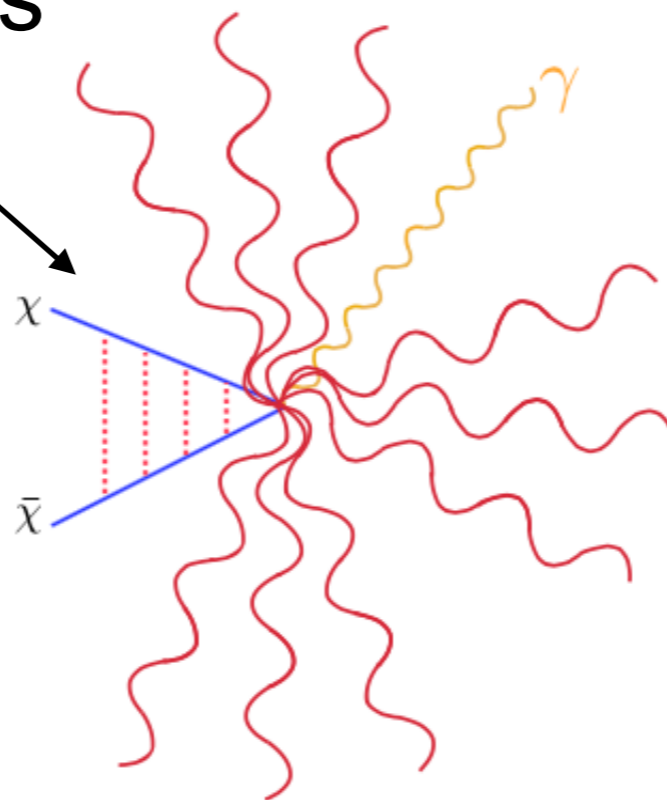
we recover these previous cases as limits

$$z \equiv E_\gamma / m_\chi$$

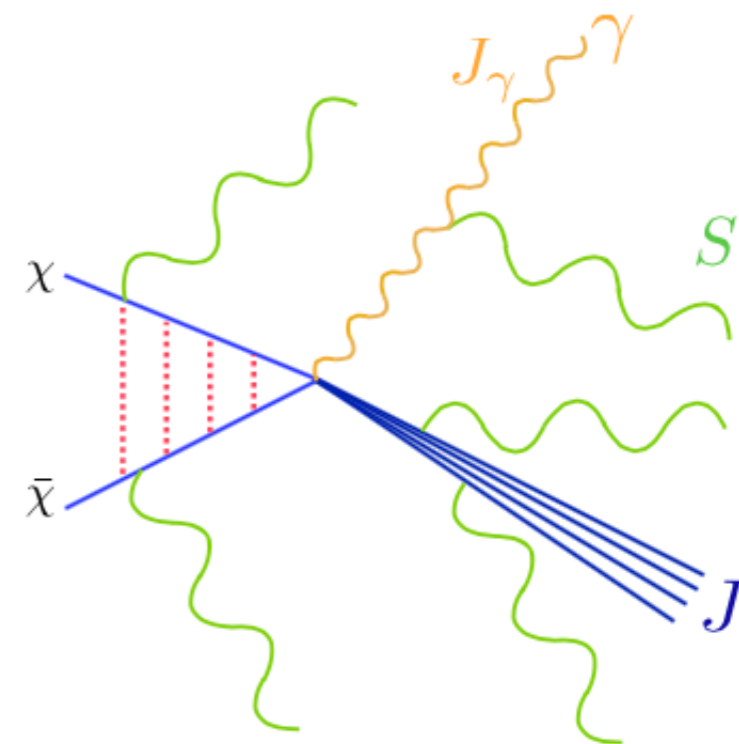
$$m_X^2 = 4m_\chi^2(1 - z)$$



(a)



(b)



(c)

Exclusive

2→2 annihilation

$\gamma\gamma, \gamma Z$ final states

Cohen et al '15; Ovanesyan, TRS & Stewart '15; Ovanesyan, Rodd, TRS & Stewart '17

Semi-inclusive

Integrate out recoil state X

$\gamma+X$ final state, X heavy

Baumgart et al '15a,b; Baumgart & Vaidya '16

Endpoint region

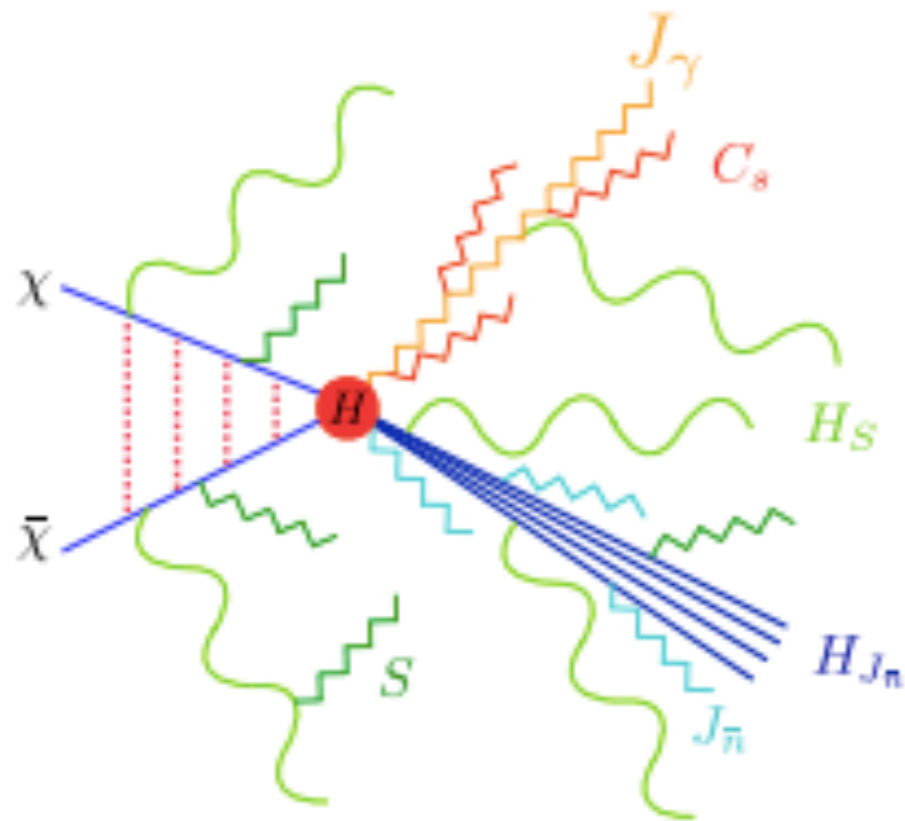
Recoil state forced into jet

$\gamma+X$ final state

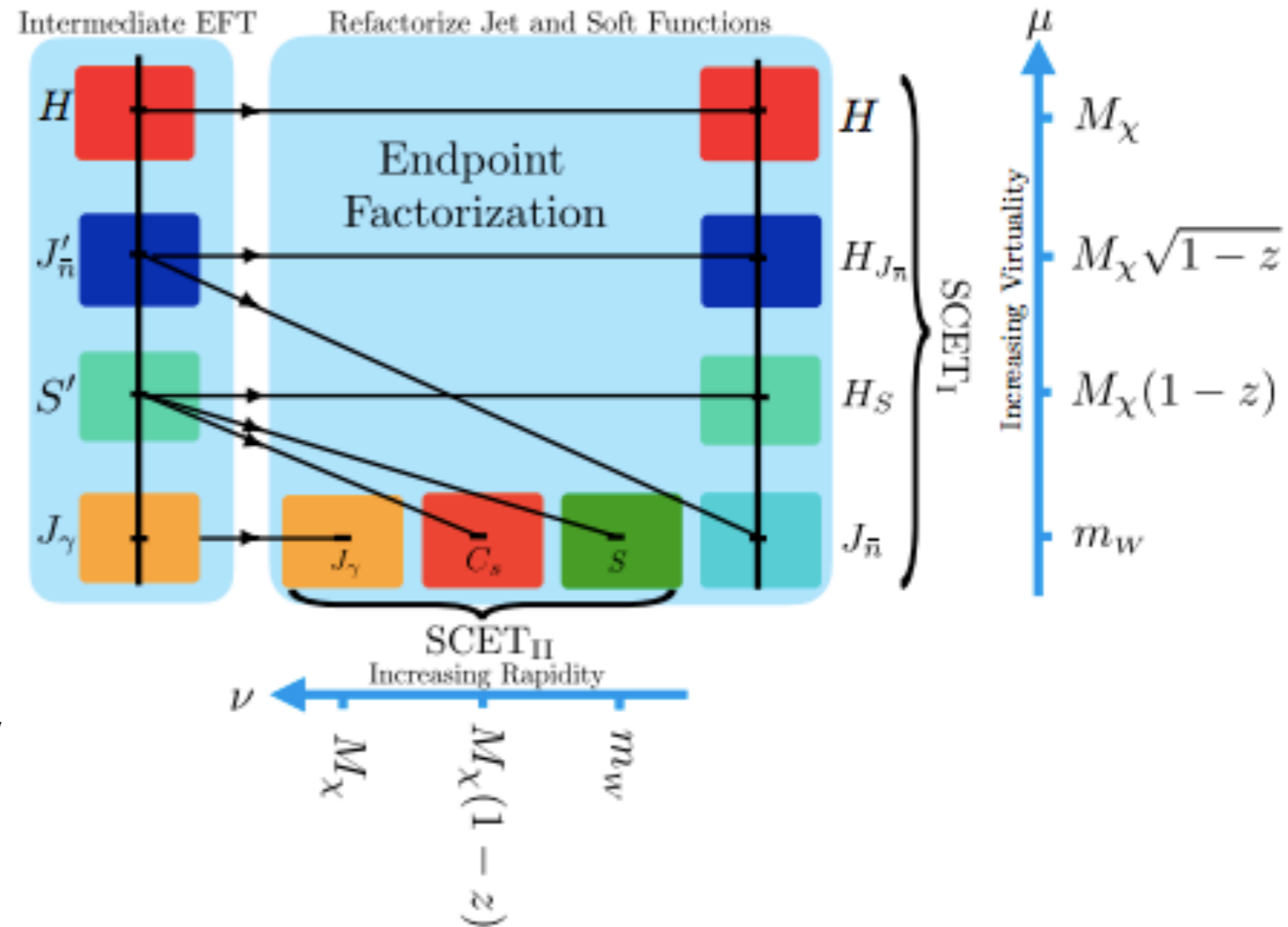
Baumgart, TRS et al, '18,'19

For the regime even closer to the endpoint, see Beneke et al '18,'19

Mode structure in the endpoint regime



curvy lines = unbroken theory
zigzag = sensitive to m_W

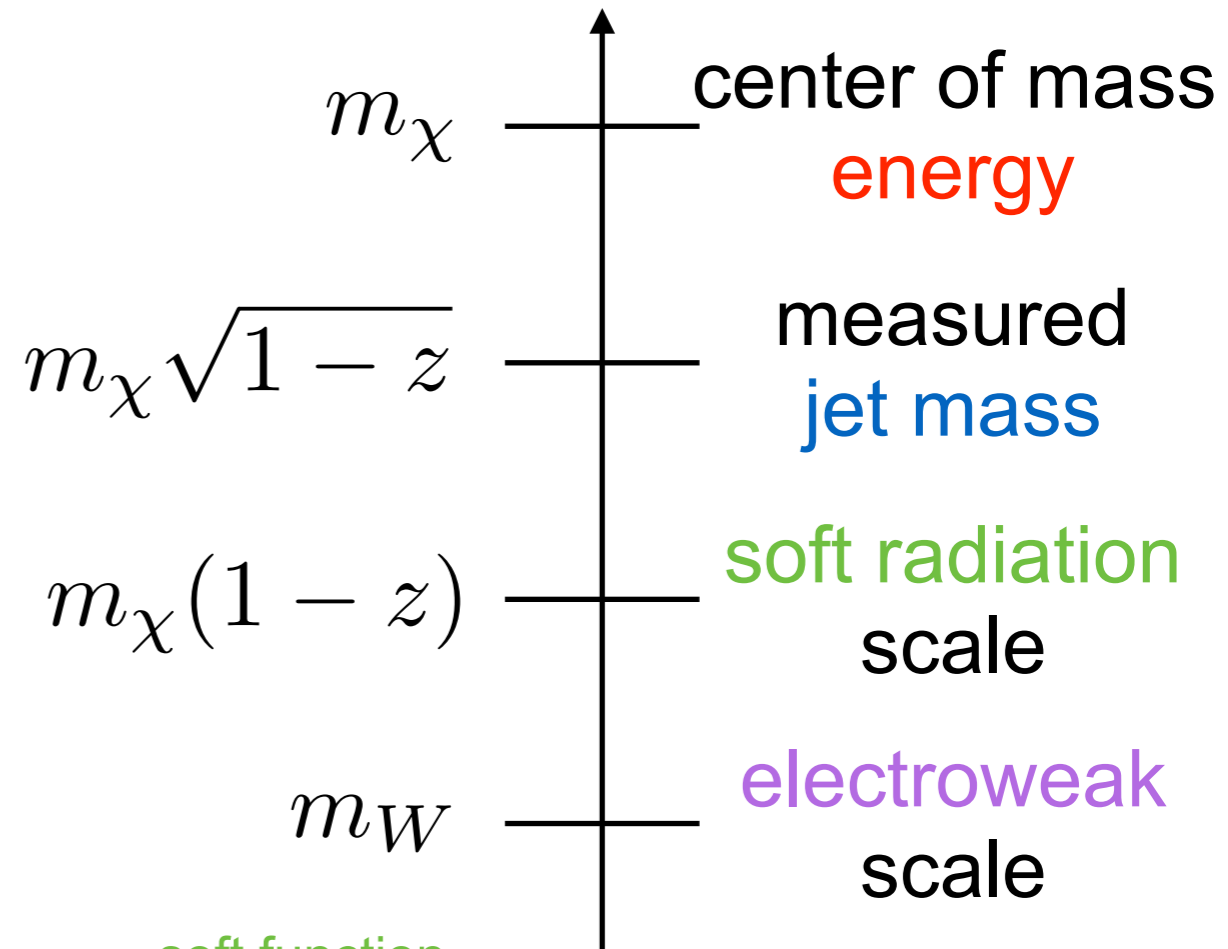


- Two relevant small scales - EW symmetry breaking (m_W) and separation from endpoint (controlled by z)
- Need two-stage factorization, modes separated by both virtuality and rapidity

Stage 1: factorization in SCET_I

- Small parameter: $\lambda = \sqrt{1 - z}$
- Using SCET_I formalism, cross section factorizes into hard, ultrasoft, collinear-jet contributions. Modes are:

$$p_c \sim M_\chi(1, \lambda^2, \lambda), \quad p_{us} \sim M_\chi(\lambda^2, \lambda^2, \lambda^2)$$



$$\frac{d\hat{\sigma}}{dz} = \underbrace{H_{ij}(M_\chi)}_{\text{hard function}} \underbrace{J_\gamma(m_W)}_{\text{photon jet function}} \underbrace{J'_{\bar{n}}(M_\chi, 1 - z, m_W)}_{\text{recoiling jet function}} \otimes \underbrace{S'_{ij}(1 - z, m_W)}_{\text{soft function}}$$

- Still need to disentangle scale dependences in soft function and jet function, break into modes with simple virtuality/rapidity scaling. Use SCET_{II} for this.

Stage 2: refactorization

- For the jet function, two types of collinear modes, corresponding to the two low scales; allows factorization of jet function into (piece depending on z) \times (piece depending on m_W).

$$J'_{\bar{n}}(M_\chi, \sqrt{1-z}, m_W, \mu) = H_{J_{\bar{n}}}(M_\chi, \sqrt{1-z}, \mu) J_{\bar{n}}(m_W, \mu, \nu) + \mathcal{O}\left(\frac{m_W}{M_\chi \sqrt{1-z}}\right)$$

- Soft function is more complicated - collinear-soft modes are required to capture all divergences:

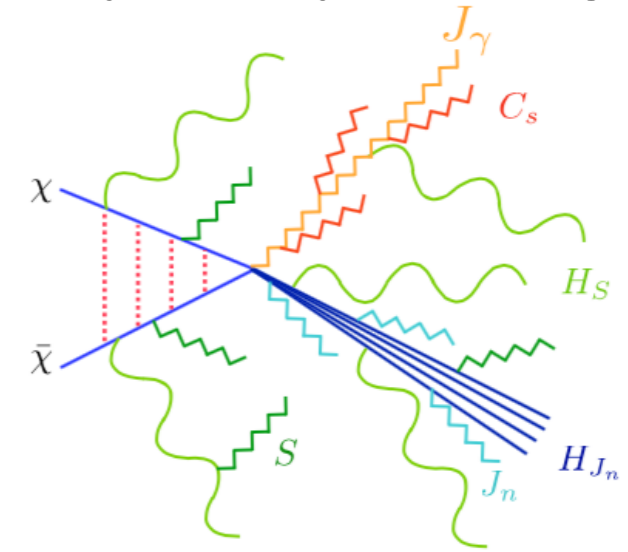
$$p_{cS} \sim M_\chi(1-z)(\lambda^2, 1, \lambda), \quad \lambda = \frac{m_W}{M_\chi(1-z)}.$$

- Hilbert space factorizes into soft (with $\lambda=m_W/m_\chi$) and collinear-soft modes (the latter scaling with both m_W and z).

$$S'_i{}^{aba'b'}(M_\chi, 1-z, m_W) = H_{S,ij}(M_\chi, 1-z, \mu) \left[C_S(M_\chi, 1-z, m_W, \mu, \nu) S(m_W, \mu) \right]_j^{aba'b'}$$

Structure of the resummed result

zigzag = modes sensitive to electroweak symmetry breaking



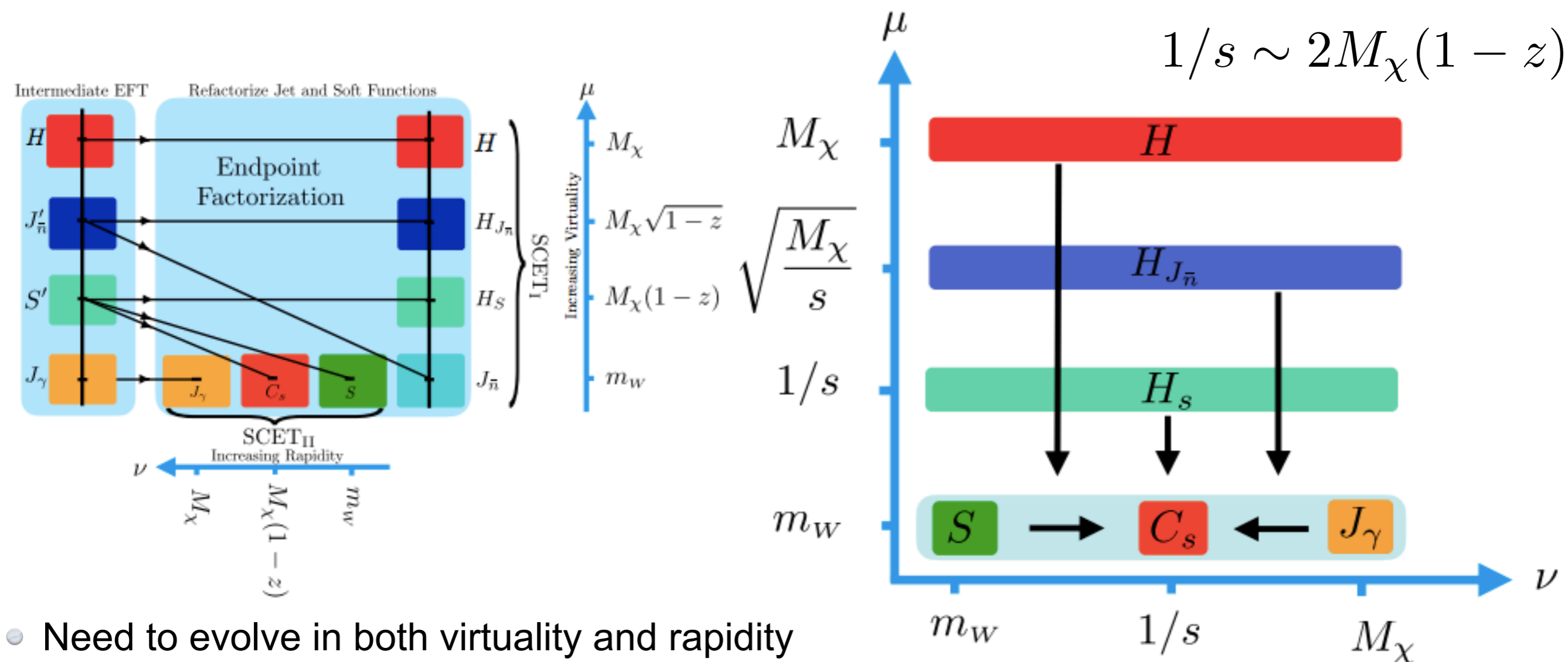
$$\left(\frac{d\hat{\sigma}}{dz}\right)^{\text{NLL}} = H(M_\chi, \mu) J_\gamma(m_W, \mu, \nu) J_{\bar{n}}(m_W, \mu, \nu) S(m_W, \mu, \nu) \\ \times H_{J_{\bar{n}}}(M_\chi, 1-z, \mu) \otimes H_S(M_\chi, 1-z, \mu) \otimes C_S(M_\chi, 1-z, m_W, \mu, \nu).$$

- We proved a factorization theorem that is valid to NLL, allowing the cross section to be separated into functions describing physics at different scales.

- $H(M_\chi, \mu)$: this hard function captures virtual corrections for $\chi\chi \rightarrow \gamma\gamma, \gamma Z$.
 - $H_{J_{\bar{n}}}(M_\chi, 1-z, \mu)$: this jet function captures the collinear radiation at the scale $M_\chi\sqrt{1-z}$.
 - $H_S(M_\chi, 1-z, \mu)$: this soft function captures soft radiation at the scale $M_\chi(1-z)$.
- do not depend on EWSB, can be evaluated in unbroken theory

- $J_\gamma(m_W, \mu, \nu)$: this photon jet function captures the virtual corrections to the outgoing γ .
 - $S(m_W, \mu, \nu)$: this soft function captures wide angle soft radiation at the electroweak scale.
 - $J_{\bar{n}}(m_W, \mu, \nu)$: this jet function captures collinear radiation in X at the electroweak scale.
 - $C_S(M_\chi, 1-z, m_W, \mu, \nu)$: this collinear-soft function captures radiation along the γ direction.
- sensitive to low scale m_W , must be evaluated in broken theory.

RG evolution path



- Need to evolve in both virtuality and rapidity
- At $\mu = m_W$, we find the relevant parts (for NLL) of the rapidity anomalous dimensions vanish - trivial to evolve in rapidity at $\mu = m_W$
- Simplest path thus runs $H/H_{J_n}/H_s$ functions down to $\mu \sim m_W$, then rapidity evolution to $\nu \sim 1/s$ is trivial

Schematic form for general representations

$$\frac{d\sigma}{dz} = \sum_{a'b'ab} F_{\chi}^{a'b'ab} \frac{d\hat{\sigma}^{a'b'ab}}{dz},$$

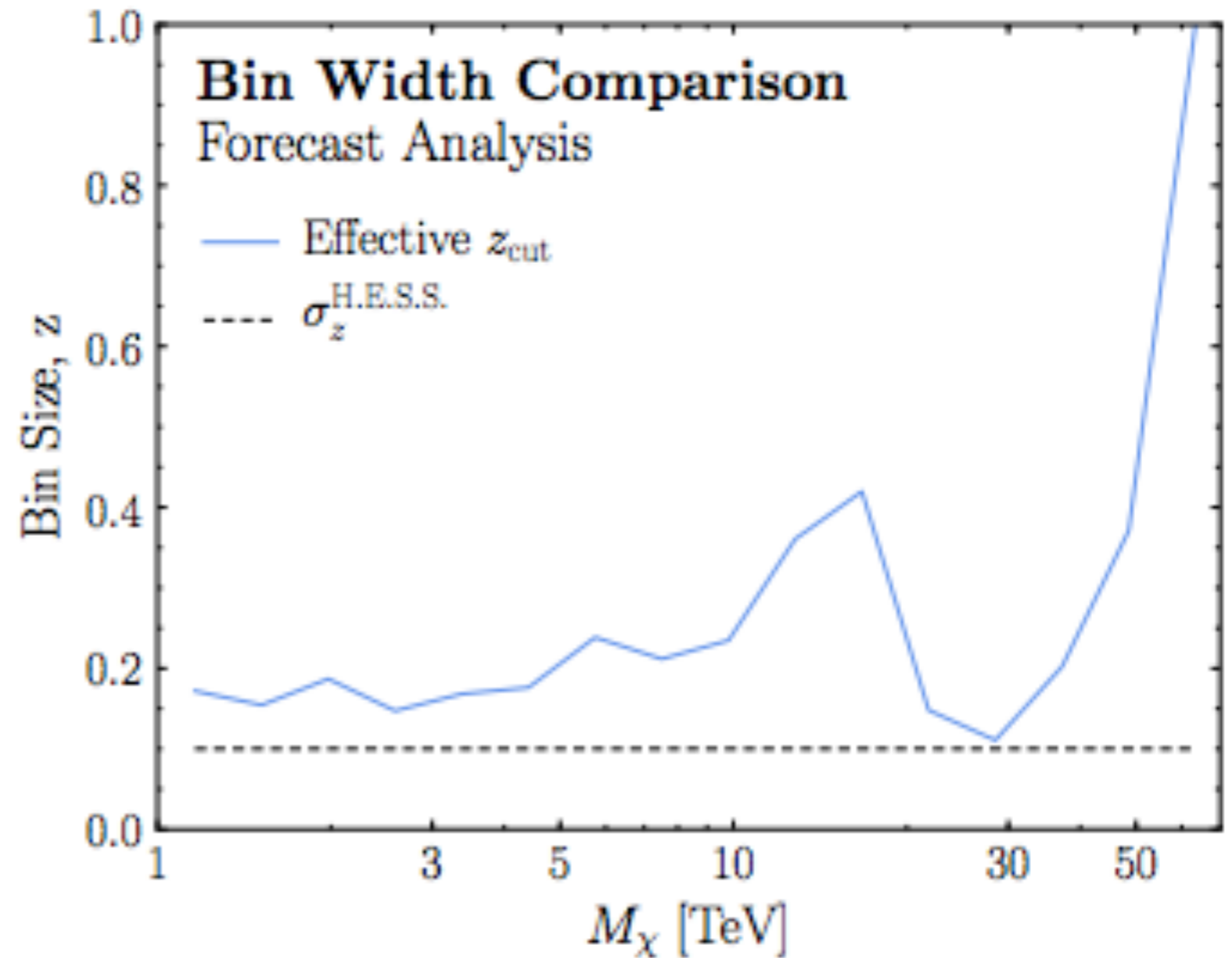
$$F_{\chi}^{a'b'ab} = \langle (\chi^0 \chi^0)_S | \left(\chi_v^T i\sigma_2 \{t_{\chi}^{a'}, t_{\chi}^{b'}\} \chi_v \right)^{\dagger} | 0 \rangle \langle 0 | \left(\chi_v^T i\sigma_2 \{t_{\chi}^a, t_{\chi}^b\} \chi_v \right) | (\chi^0 \chi^0)_S \rangle.$$

$$\begin{aligned} \left(\frac{d\hat{\sigma}}{dz} \right)^{\text{NLL}} &= H(M_{\chi}, \mu) J_{\gamma}(m_W, \mu, \nu) J_{\bar{n}}(m_W, \mu, \nu) S(m_W, \mu, \nu) \\ &\quad \times H_{J_{\bar{n}}}(M_{\chi}, 1-z, \mu) \otimes H_S(M_{\chi}, 1-z, \mu) \otimes C_S(M_{\chi}, 1-z, m_W, \mu, \nu), \end{aligned}$$

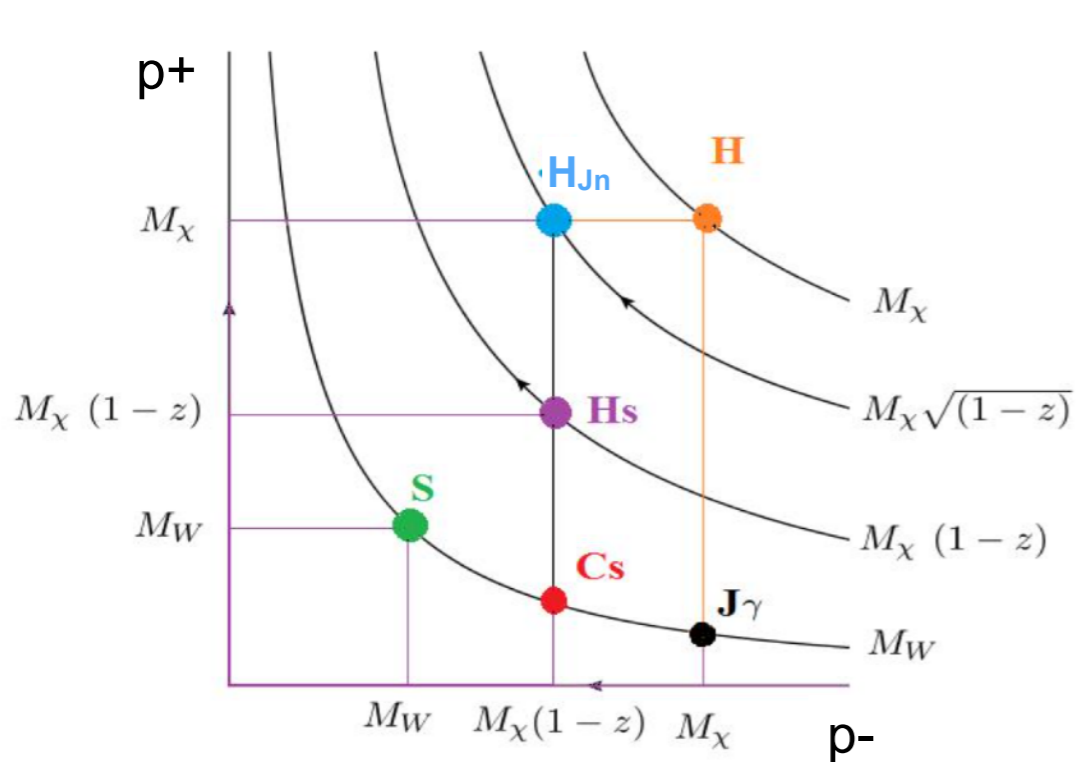
- F captures Sommerfeld factors (representation-dependent)
- Remaining pieces capture representation-independent factorized structure of cross section valid at NLL

An aside

- From earlier: it is not sufficient to model energy resolution as counting photons in a bin of specified width
- If we modeled the spectrum as a line with intensity given by # photons in a bin - what would the bin width need to be to get the correct constraint (from full spectrum analysis)?
- Required bin width varies at the O(1) level as a function of DM mass



Rapidity renormalization



- “Virtuality” $\sim \sqrt{p^2} \sim Q \lambda$ for collinear and soft modes, $Q \lambda^2$ for ultrasoft modes - compare to usual regulating parameter μ appearing in RG evolution.
- But in SCET_{II}, collinear and soft modes have same virtuality / invariant mass - can be exchanged by a boost, distinguished only by their rapidity.

- Can’t use running in virtuality to capture large logs between soft and collinear scales. Instead these logs arise from “rapidity divergences” - need to introduce “rapidity renormalization group” to resum them [Chiu et al ’12].
- Introduce new (boost-violating) regularization parameter v .
- Natural scale of v (minimizing logs) is $\sim Q$ for collinear modes, $Q \lambda$ for soft modes, $Q \lambda^2$ for ultrasoft.
- Collinear-soft modes have natural scales $\mu \sim m_W$, $v \sim m_\chi(1-z)$.

RG evolution

anomalous dimensions

$$\gamma_{\mu,ij}^H = -2 C_2 \frac{\alpha_W}{\pi} \log \left(\frac{\mu^2}{(2 M_\chi)^2 z} \right) \delta_{ij}$$

$$\gamma_\mu^{H_{J\bar{n}}} = 2 C_2 \frac{\alpha_W}{\pi} \log \left(\frac{\mu^2 s}{2 M_\chi} \right)$$

$$\frac{d}{d \log \mu} H_{S,11} = 0, \quad \frac{d}{d \log \mu} H_{S,ij} = \gamma_{\mu,jk}^{H_S} H_{S,ik}$$

$$\frac{d}{d \log \mu} H_{S,33} = -3 C_2 \frac{\alpha_W}{\pi} \log(\mu s) H_{S,33},$$

$$\frac{d}{d \log \mu} H_{S,31} = 2 C_2 \frac{\alpha_W}{\pi} \log(\mu s) H_{S,33},$$

$$\frac{d}{d \log \mu} H_{S,22} = -3 C_2 \frac{\alpha_W}{\pi} \log(\mu s) H_{S,22},$$

$$\frac{d}{d \log \mu} H_{S,24} = C_2 \frac{\alpha_W}{\pi} \log(\mu s) H_{S,22}.$$

evolution kernels

$$U_H(2M_\chi, m_W) = \exp \left(-2 C_2 \frac{\alpha_W}{\pi} \log^2 \left(\frac{m_W}{2 M_\chi} \right) \right),$$

$$U_{H_{J\bar{n}}} \left(\sqrt{2M_\chi/s}, m_W \right) = \exp \left(2 C_2 \frac{\alpha_W}{\pi} \log^2 \left(m_W \sqrt{\frac{s}{2 M_\chi}} \right) \right),$$

$$H_{S,11}(m_W) = H_{S,11}(1/s),$$

$$\begin{pmatrix} H_{S,33}(m_W) \\ H_{S,31}(m_W) \end{pmatrix} = \begin{pmatrix} U_{H_S} & 0 \\ 2(1 - U_{H_S})/3 & 1 \end{pmatrix} \begin{pmatrix} H_{S,33}(1/s) \\ H_{S,31}(1/s) \end{pmatrix},$$

$$\begin{pmatrix} H_{S,22}(m_W) \\ H_{S,24}(m_W) \end{pmatrix} = \begin{pmatrix} U_{H_S} & 0 \\ (1 - U_{H_S})/3 & 1 \end{pmatrix} \begin{pmatrix} H_{S,22}(1/s) \\ H_{S,24}(1/s) \end{pmatrix},$$

$$U_{H_S} = \exp \left(-\frac{3}{2} C_2 \frac{\alpha_W}{\pi} \log^2(m_W s) \right)$$

Limiting cases

Plus functions defined by: $\int_0^\infty dq \left(\frac{\ln(\frac{q}{U})}{q} \right)_+ F(q) = \int_U^\infty dq \left(\frac{\ln(\frac{q}{U})}{q} \right) F(q)$

\mathcal{L}_1^S cuts off for $z > 1 - \frac{m_W}{2m_\chi}$

\mathcal{L}_1^J cuts off for $z > 1 - \left(\frac{m_W}{2m_\chi} \right)^2$

separation between line and continuum regimes

Thus if we integrate from $z = 1 - \left(\frac{m_W}{2m_\chi} \right)^2$ to 1, only the line contributes:

$$\frac{d\sigma}{dz} = 4 |s_{0\pm}|^2 \sigma^{\text{tree}} e^{-2\Gamma_0 \tilde{\alpha}_W L_\chi^2} \delta(1 - z)$$

matches exclusive result from Ovanesyan et al '15, Cohen et al '15

If we integrate from 0 to 1, we recover the semi-inclusive result:

$$\int_0^1 dz \frac{d\sigma}{dz} = \frac{\pi \alpha_W^2 \sin^2 \theta_W}{2M_\chi^2 v} \left\{ \frac{4}{3} |s_{00}|^2 f_- + 2 |s_{0\pm}|^2 f_+ + \frac{2\sqrt{2}}{3} (s_{00} s_{0\pm}^* + c.c.) f_- \right\}$$

$$f_\pm = 1 \pm e^{-\frac{3}{2}\Gamma_0 \tilde{\alpha}_W L_\chi^2}$$

matches Baumgart et al '15

- Gauge invariant gauge boson operator: $\mathcal{B}_n^\mu(x) = \frac{1}{g} \left[W_n^\dagger(x) iD_{n\perp}^\mu W_n(x) \right]$

- Collinear Wilson line: $W_n = \left[\sum_{\text{perms}} \exp \left(-\frac{g}{\bar{n} \cdot \mathcal{P}} \bar{n} \cdot A_n(x) \right) \right]$

- Ultrasoft Wilson line: $Y_n^{(r)}(x) = \mathbf{P} \exp \left[ig \int_0^{\infty} ds n \cdot A_{us}^a(x + sn) T_{(r)}^a \right]$

- Soft Wilson line: $S_n^{(r)}(x) = \mathbf{P} \exp \left[ig \int_{-\infty}^0 ds n \cdot A_s^a(x + sn) T_{(r)}^a \right]$

- Collinear-soft Wilson lines:

$$X_n^{(r)}(x) = \mathbf{P} \exp \left[ig \int_{-\infty}^0 ds n \cdot A_{cs}^a(x + sn) T_{(r)}^a \right] \quad V_n^{(r)}(x) = \mathbf{P} \exp \left[ig \int_{-\infty}^0 ds \bar{n} \cdot A_{cs}^a(x + s\bar{n}) T_{(r)}^a \right]$$

- Hard Lagrangian / hard function:

$$\mathcal{L}_{\text{hard}}^{(0)} = \sum_{r=1}^2 C_r(M_\chi, \mu) \left(\chi_v^{aT} i\sigma_2 \chi_v^b \right) \left(Y_r^{abcd} \mathcal{B}_{n\perp}^{ic} \mathcal{B}_{\bar{n}\perp}^{jd} \right) i \epsilon^{ijk} (n - \bar{n})^k \quad H_{ij} = C_i C_j$$

$$Y_1^{abcd} = \delta^{ab} \left(Y_n^{ce} S_{\bar{n}}^{de} \right), \quad Y_2^{abcd} = \left(Y_v^{ae} Y_n^{ce} \right) \left(Y_v^{bf} Y_{\bar{n}}^{df} \right) \quad C_1(\mu) = -C_2(\mu) = -\pi \frac{\alpha_2(\mu)}{M_\chi}$$

- Rapidity regulators:

$$S_n = \left[\sum_{\text{perms}} \exp \left(-\frac{g}{n \cdot \mathcal{P}} \frac{\omega |2\mathcal{P}^z|^{-\eta/2}}{\nu^{-\eta/2}} n \cdot A_s(x) \right) \right],$$

- Soft/collinear measurement operators:

$$W_{\bar{n}} = \left[\sum_{\text{perms}} \exp \left(-\frac{g}{n \cdot \mathcal{P}} \frac{\omega^2 |n \cdot \mathcal{P}|^{-\eta/2}}{\nu^{-\eta/2}} n \cdot A_{\bar{n}}(x) \right) \right],$$

$$\widehat{\mathcal{M}}_s |X_s\rangle = \frac{2}{4M_\chi} \sum_{i \in X_s} n \cdot p_i |X_s\rangle, \quad \widehat{\mathcal{M}}_c |X_c\rangle = \frac{1}{4M_\chi^2} \left(\sum_{i \in X_c} p_i^\mu \right)^2 |X_c\rangle, \quad \widehat{\mathcal{M}}_{c_s} |X_{c_s}\rangle = \frac{2}{4M_\chi} \sum_{i \in X_{c_s}} \bar{n} \cdot p_i |X_{c_s}\rangle$$

- Soft functions: $S'_{ij}(1 - z_s, m_W) = \langle 0 | \bar{\text{T}} Y_i^\dagger(0) \delta((1 - z_s) - \widehat{\mathcal{M}}_s) \text{T} Y_j(0) | 0 \rangle$

- Collinear/soft function: $\tilde{S}_j^{aba'b'} = (C_S S)_j^{aba'b'}$

$$C_S(M_\chi, 1 - z_c, m_W, \mu, \nu) = \langle 0 | (X_n V_n)^\dagger \delta((1 - z_c) - \widehat{\mathcal{M}}_{c_s}) X_n V_n | 0 \rangle$$

$$\tilde{S}_1^{aba'b'} = \langle 0 | \left(Y_n^{3f'} Y_{\bar{n}}^{dg'} \right)^\dagger \delta((1 - z_s) - \widehat{\mathcal{M}}_{c_s}) \left(Y_n^{3f} Y_{\bar{n}}^{dg} \right) | 0 \rangle \delta^{f'g'} \delta^{a'b'} \delta^{fg} \delta^{ab},$$

$$\tilde{S}_2^{aba'b'} = \langle 0 | \left(Y_n^{ce} Y_{\bar{n}}^{Ae} \right)^\dagger \delta((1 - z_s) - \widehat{\mathcal{M}}_{c_s}) Y_n^{c'g'} Y_{\bar{n}}^{A'g'} | 0 \rangle \langle 0 | \left[S_n^{3c} S_n^{3c'} S_v^{a'A'} S_v^{aA} \right] | 0 \rangle \delta^{bb'},$$

$$\begin{aligned} \tilde{S}_3^{aba'b'} &= \langle 0 | \left(Y_n^{ce} Y_{\bar{n}}^{B'e} \right)^\dagger \delta((1 - z_s) - \widehat{\mathcal{M}}_{c_s}) Y_n^{c'g'} Y_{\bar{n}}^{A'g'} | 0 \rangle \\ &\times \left(\langle 0 | \left[S_n^{3c} S_n^{3c'} S_v^{a'A'} S_v^{b'B'} \right] | 0 \rangle \delta^{ab} + \langle 0 | \left[S_n^{3c} S_n^{3c'} S_v^{aA'} S_v^{bB'} \right] | 0 \rangle \delta^{a'b'} \right). \end{aligned} \quad (4.28)$$

Tree-level functions

hard and hard-soft
functions

$$H_{11} = 1, \quad H_{22} = 1, \quad H_{12} = H_{21} = -1$$

$$H_{S,11} = 1, \quad H_{S,22} = 2, \quad H_{S,33} = 1$$

combined collinear-soft + soft function

$$\tilde{S}_j^{aba'b'} = (C_S S)_j^{aba'b'}$$

$$\tilde{S}_1^{aba'b'} = \delta^{a'b'} \delta^{ab},$$

$$\tilde{S}_2^{aba'b'} = \delta^{a3} \delta^{a'3} \delta^{bb'},$$

$$\tilde{S}_3^{aba'b'} = \delta^{a3} \delta^{b3} \delta^{a'b'} + \delta^{a'3} \delta^{b'3} \delta^{ab},$$

$$\tilde{S}_4^{aba'b'} = \delta^{a'a} \delta^{bb'}.$$

- Jet functions:

$$J_{\bar{n}}^{dd'}(M_\chi, 1 - z_c, m_W) = \langle 0 | B_{\bar{n}\perp}^{d'} \delta((1 - z_c) - \widehat{\mathcal{M}}_c) \delta(M_\chi - \bar{n} \cdot \mathcal{P}) \delta^2(\vec{\mathcal{P}}_\perp) B_{\bar{n}\perp}^d | 0 \rangle$$

$$J_\gamma(m_W) = \langle 0 | B_{\bar{n}\perp}^c | \gamma \rangle \langle \gamma | B_{\bar{n}\perp}^c | 0 \rangle,$$

- Recoiling jet function:

$$J_{\bar{n}}(k) = \delta(2M_\chi k^+) + \frac{\alpha_W}{4\pi} \left(\frac{4C_2(G) \log(2M_\chi k^+ / \mu^2) - \beta_0}{2M_\chi k^+} \right)_+$$

- Photon jet function:

$$J_{\bar{n}}^{(0)} = -2,$$

$$J_{\bar{n}}^{(1)} = -2C_2 \frac{\alpha_W}{\pi} \left(\frac{\mu}{M} \right)^{2\epsilon} \left(\frac{\nu}{2E_\gamma} \right)^\eta \frac{\Gamma(\epsilon)}{\eta} \\ + \frac{\alpha_W}{2\pi} \Gamma(\epsilon) \left(\frac{\mu}{M} \right)^{2\epsilon} \left[\frac{11}{3} C_2 - \frac{4}{3} n_f C(R) \right]$$

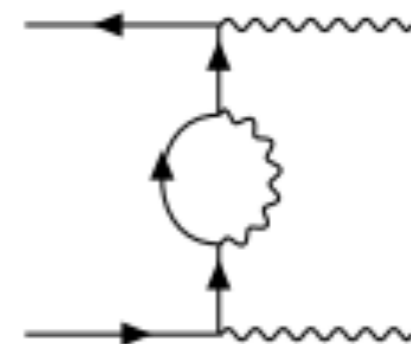
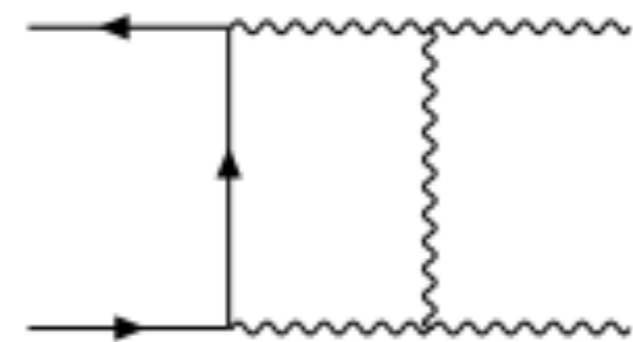
Beyond LL: high-scale matching

- At NLL, only tree-level high-scale matching is needed. For NLL', we have performed it at one-loop.
- Compute (25) one-loop diagrams in the full theory, match onto SCET_{EW} operators. We provide analytic expressions graph-by-graph [appendix A of Ovanesyan, Rodd, TRS & Stewart '16].

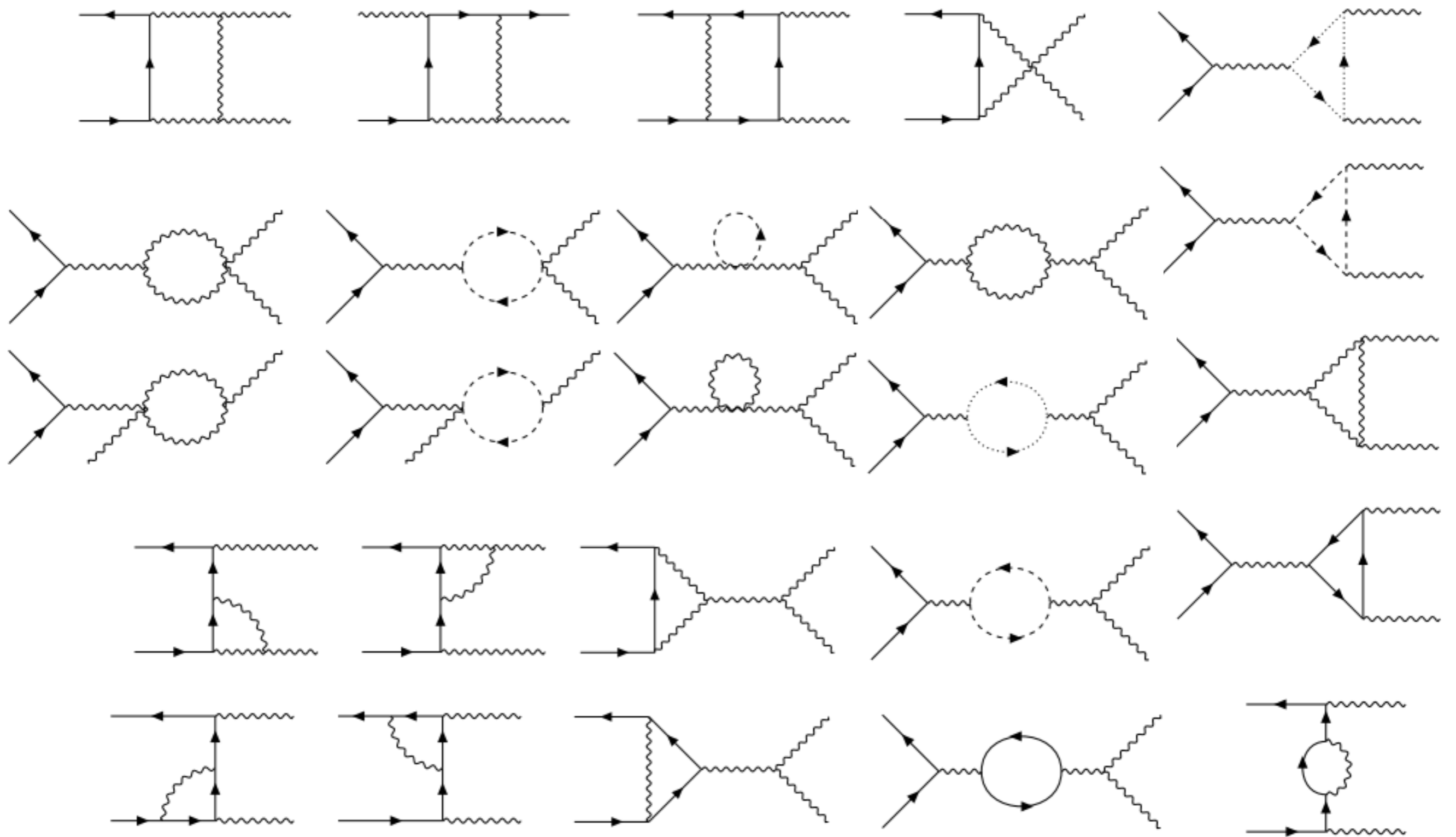
$$C_1(\mu) = -\frac{\pi\alpha_2(\mu)}{m_\chi} + \frac{\alpha_2(\mu)^2}{4m_\chi} \left[2 \ln^2 \frac{\mu^2}{4m_\chi^2} + 2 \ln \frac{\mu^2}{4m_\chi^2} + 2i\pi \ln \frac{\mu^2}{4m_\chi^2} + 8 - \frac{11\pi^2}{6} \right],$$

$$C_2(\mu) = \frac{\pi\alpha_2(\mu)}{m_\chi} - \frac{\alpha_2(\mu)^2}{2m_\chi} \left[\ln^2 \frac{\mu^2}{4m_\chi^2} + 3 \ln \frac{\mu^2}{4m_\chi^2} - i\pi \ln \frac{\mu^2}{4m_\chi^2} - \frac{5\pi^2}{12} \right].$$

example diagrams



High-scale matching diagrams



Beyond LL: low-scale matching

- At NLL, only tree-level low-scale matching + log piece of one-loop matching is needed. For NLL', we have performed the full matching at one-loop.
- Compute one-loop diagrams that appear in SCET_{EW} but not SCET_γ , match onto SCET_γ operators after electroweak symmetry breaking.

$$\exp \left[\hat{D}^X(\mu) \right] = \left[\hat{D}_s(\mu) \right] \left[D_c^X(\mu) \mathbb{I} \right] \exp \left[\sum_{i \in X} D_c^i(\mu) \mathbb{I} \right]$$

X labels final state $\gamma\gamma, \gamma Z, ZZ$

non-diagonal
matrix from soft
interactions

initial state
diagonal
contribution

final state diagonal
contribution

$$\hat{D}_s = \begin{pmatrix} 1 + \frac{\alpha_2(\mu)}{2\pi} \left[\ln \frac{m_W^2}{\mu^2} (1 - 2i\pi) + c_W^2 \ln \frac{m_Z^2}{\mu^2} \right] & \frac{\alpha_2(\mu)}{2\pi} \ln \frac{m_W^2}{\mu^2} (1 - i\pi) \\ 1 + \frac{\alpha_2(\mu)}{2\pi} \ln \frac{m_W^2}{\mu^2} (2 - 2i\pi) & 1 \end{pmatrix}$$

contribution
needed for NLL

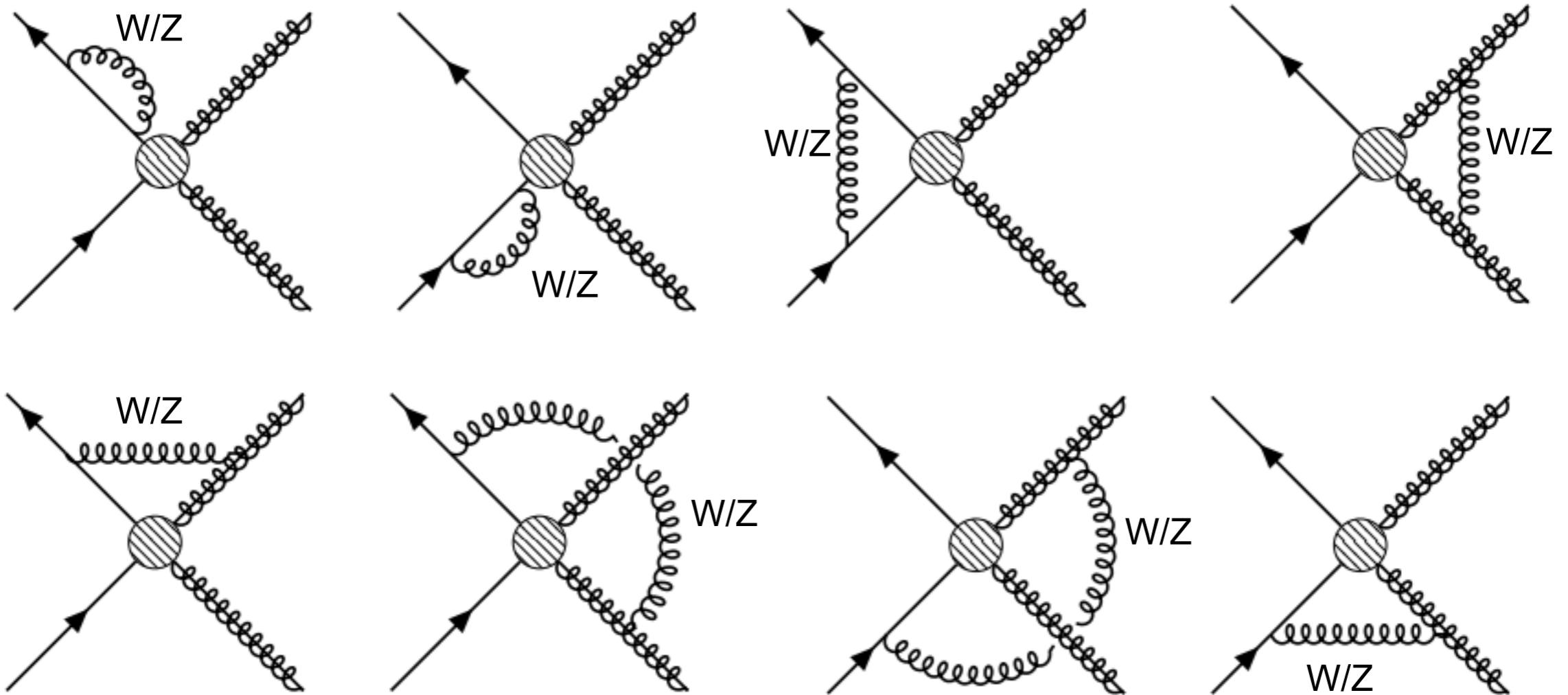
$$D_c^i(\mu) = \frac{\alpha_2(\mu)}{2\pi} \left[\ln \frac{m_W^2}{\mu^2} \ln \frac{4m_\chi^2}{\mu^2} - \frac{1}{2} \ln^2 \frac{m_W^2}{\mu^2} \right.$$

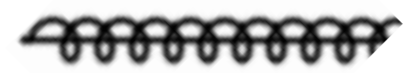
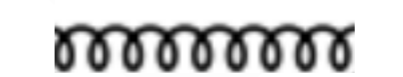
finite constants
dependent on final state

$$\left. - \ln \frac{m_W^2}{\mu^2} + c_1^i \ln \frac{m_Z^2}{\mu^2} + c_2^i \right]$$

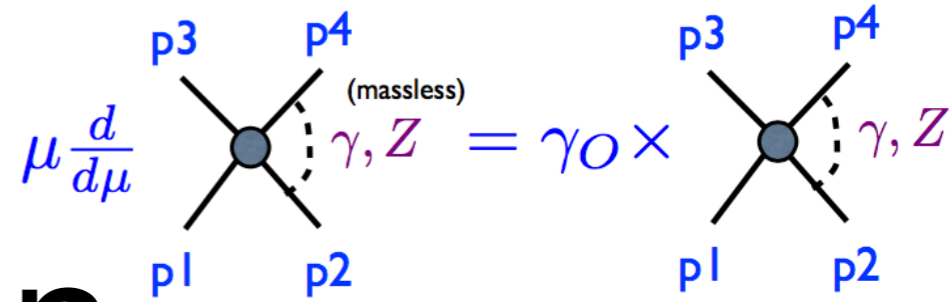
$$D_c^X(\mu) = 1 - \frac{\alpha_2(\mu)}{2\pi} \left[\ln \frac{m_W^2}{\mu^2} + c_W^2 \ln \frac{m_Z^2}{\mu^2} \right]$$

Low-scale matching diagrams



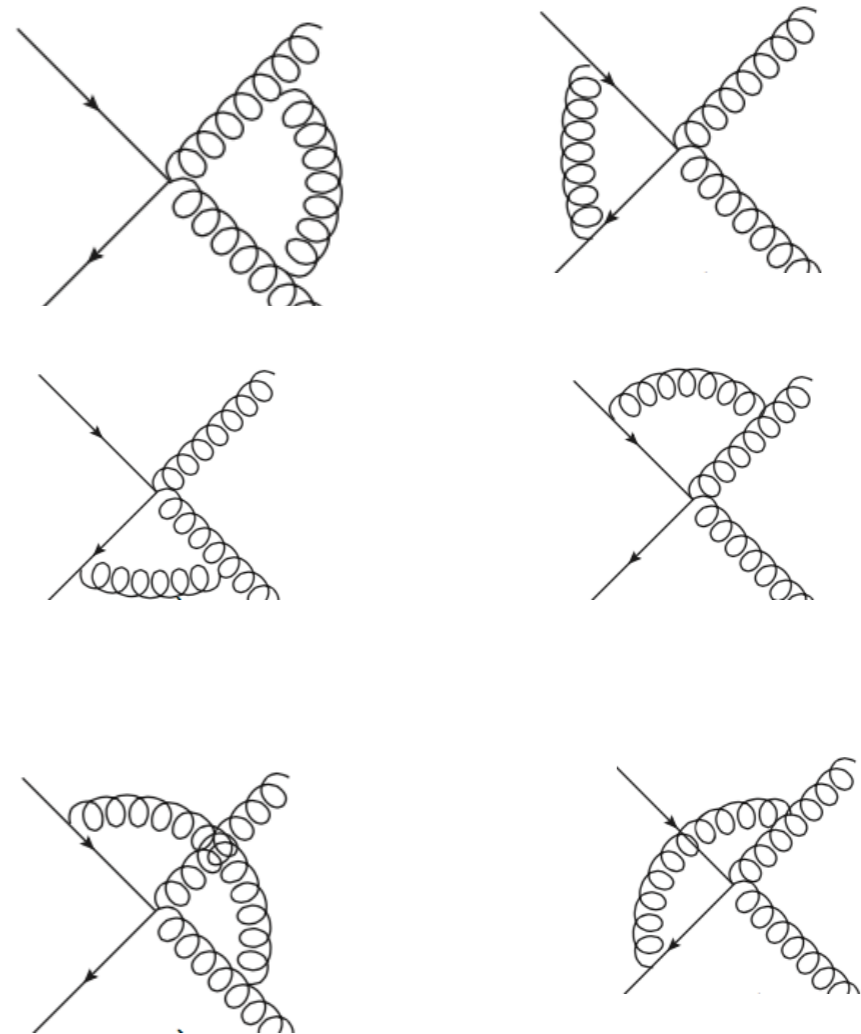
 collinear gauge bosons
 soft gauge bosons

Beyond LL: the anomalous dimension



- Novel feature of this case: incoming particles are non-relativistic, momentum 4-vectors in same direction $v = (1,0,0,0)$. Gives rise to soft S_v Wilson lines that can interact with each other or themselves.
- Anomalous dimension has two contributions:
 - Collinear piece, must be calculated to 2-loop for NLL, but is unchanged from case with lightlike incoming particles - can use results in literature [Chiu et al '09].
 - Soft piece - needs to be recalculated, but only at one-loop [Ovanesyan, TRS & Stewart '15].

Diagrams for soft anom. dim.



+wavefunction renormalization

$$\hat{\gamma} = 2\gamma_{W_T} \mathbb{I} + \hat{\gamma}_S \quad \Gamma_1^g = 8 \left(\frac{70}{9} - \frac{2}{3}\pi^2 \right)$$

$$\gamma_{W_T} = \frac{\alpha_2}{4\pi} \Gamma_0^g \ln \frac{2m_\chi}{\mu} - \frac{\alpha_2}{4\pi} b_0 + \left(\frac{\alpha_2}{4\pi} \right)^2 \Gamma_1^g \ln \frac{2m_\chi}{\mu}$$

$$\hat{\gamma}_S^{\text{NLL}} = \frac{\alpha_2}{\pi} (1 - i\pi) \begin{pmatrix} 2 & 1 \\ 0 & -1 \end{pmatrix} - \frac{2\alpha_2}{\pi} \begin{pmatrix} 1 & 0 \\ 0 & 1 \end{pmatrix}$$

The analysis

- 2D binned likelihood analysis in position (ROI #) and energy, to exploit knowledge of DM spectrum/distribution.
- Spatial bins are concentric rings, 0.1 degrees wide (masked areas removed).
- Default analysis is within 1 degree radius of GC: 7 Regions of Interest (ROIs), as region within 0.3 degrees of plane is masked.
- Also consider observations with up to 4 degree radius (37 ROIs total).

